

**STABILIZATION OF SONO SYNTHESIZED  
PHOTOCATALYST ON TEXTILES AND DEVELOPMENT OF  
MULTIFUNCTIONAL NANOCOMPOSITES**

**Muhammad Tayyab Noman, M.Sc.**

**SUMMARY OF THE THESIS**

### **Committee for the defense of the dissertation:**

předseda:

doc. Ing. Michal Vik, Ph.D.

FT TUL, katedra materiálového inženýrství

místopředseda:

prof. Ing. Josef Šedlbauer, Ph.D.

FP TUL, katedra chemie

prof. Dr. Ing. Miroslav Černík, CSc. (oponent)

FM TUL, Ústav nových technologií a aplikované informatiky

doc. Ing. Ladislav Burgert, CSc. (oponent)

Univerzita Pardubice, FCHT, odd. syntetických polymerů, vláken a text. chemie

doc. Ing. Petr Exnar, CSc.

FP TUL, katedra chemie

doc. Ing. Antonín Kuta, CSc.

VŠCHT, Fakulta chemicko-technologická, Ústav polymerů

doc. Mgr. I. Lovětinská-Šlamborová, Ph.D.

FP TUL, katedra chemie

Ing. Michal Černý, Ph.D.

Univerzita Pardubice, FCHT, odd. synt. polymerů, vláken a textilní chemie

Ing. Blanka Tomková, Ph.D.

FT TUL, katedra materiálového inženýrství

Field of study: Textile Technics and Materials Engineering.

Supervisor: Ing. Jana Šašková, Ph.D., guarantor: prof. Ing. Jakub Wiener, Ph.D.

The dissertation is available at the Dean's Office FT TUL.

Liberec 2019

## **Abstract**

Nanoparticles (NPs) with smaller size and higher crystallinity exert a remarkable influence on the photocatalytic performance of a photocatalyst. This dissertation is about the synthesis and stabilization of a novel photocatalyst to enhance the functional properties of textiles. Moreover, an in-situ Ultrasonic Acoustic Method (UAM) is used to develop novel Cotton-TiO<sub>2</sub> (CT) multifunctional nanocomposites.

Highly photo active pure anatase form of TiO<sub>2</sub> (titanium dioxide, titania) NPs with average particle size 4 nm have been successfully synthesized by Ultrasonic Acoustic Method (UAM). The effects of process variables i.e. precursors concentration and sonication time were investigated based on Central Composite Design (CCD) and Response Surface Methodology (RSM). The characteristics of the Resulting Nanoparticles (RNP) were analysed by Scanning Electron Microscopy (SEM), Dynamic Light Scattering (DLS), Transmission Electron Microscopy (TEM), X-ray Diffractometry (XRD) and Raman Spectroscopy. Photocatalytic experiments were performed with Methylene Blue (MB) dye which is considered as a model organic pollutant in textile industry. A comparative analysis between the developed photocatalyst and commercially available photocatalyst Degussa P25 was performed for photocatalytic performance against dye removal efficiency. The rapid removal of MB in case of RNP indicates their higher photocatalytic activity than P25. Maximum dye removal efficiency 99 % was achieved with optimal conditions i.e. Titanium Tetraisopropoxide (TTIP) conc. 10 mL, Ethylene Glycol (EG) conc. 4 mL and sonication time 1 h. Interestingly, no significant difference was found in the photocatalytic performance of RNP after calcination. Moreover, self-cleaning efficiency of RNP deposited on cotton was evaluated in RGB (Red, Green, Blue) colour space. The obtained results indicate the significant impact of ultrasonic irradiations on the photocatalytic performance of pure anatase form than any other hybrid type of TiO<sub>2</sub> NPs.

In another experiment, facile embedding of the Resulting Nanoparticles (RNP) onto cotton fabric has been successfully attained by Ultraviolet (UV) light irradiations. The adhesion of NPs with fibre surface, tensile behaviour and physicochemical changes before and after UV treatment were investigated by SEM, Energy Dispersive X-ray (EDX) and Inductive Couple Plasma-Atomic Emission (ICP-AES) Spectroscopies. Experimental variables i.e. dosage of TiO<sub>2</sub> NPs, temperature of the system and time of UV irradiations were optimised by CCD and RSM. Moreover, two different mathematical models were developed for incorporated TiO<sub>2</sub> onto cotton and tensile strength of cotton after UV treatment, and further used to testify the obtained results. Self-clean fabric through a synergistic combination of cotton with highly photo active TiO<sub>2</sub> NPs was produced. Stability against UV irradiations and self-cleaning properties of the produced fabric were evaluated.

Finally, Cotton-TiO<sub>2</sub> (CT) nanocomposites with multifunctional properties were synthesized by an in-situ Ultrasonic Acoustic Method (UAM). Ultrasonic irradiations were used as a potential tool to develop CT nanocomposites at low temperature in the presence of Titanium Tetrachloride (TTC) and Isopropanol (ISP). The synthesized samples were characterized by XRD, SEM, EDX and ICP-AES methods. Functional properties i.e. Ultraviolet Protection Factor (UPF), self-cleaning, washing durability, antimicrobial and tensile strength of the CT nanocomposites were evaluated by different methods. CCD and RSM were employed to evaluate the effects of selected variables on responses. The results confirm the simultaneous formation and incorporation of anatase TiO<sub>2</sub> with average crystallite size of 4 nm on cotton fabric with excellent photocatalytic properties. The sustained self-cleaning efficiency of CT nanocomposites even after 30 home launderings indicates their excellent washing durability. Significant effects were obtained during statistical analysis for selected variables on the formation and incorporation of TiO<sub>2</sub> NPs on cotton and photocatalytic properties of CT nanocomposites.

### **Keywords**

TiO<sub>2</sub>; Anatase; Photocatalysis; Sonochemical synthesis; Dyes degradation; Ultrasonic irradiations; Ethylene glycol; Response surfaces; Self-stabilization; Self-cleaning; Nanoparticles; Ultrasonic acoustic method; Ultraviolet protection factor; Nanocomposites

## **Abstrakt**

Nanočástice (NP) s menší velikostí a vyšší krystalinitou mají významný vliv na fotokatalytický výkon fotokatalyzátoru. Tato práce se zabývá syntézou a stabilizací nového fotokatalyzátoru pro zvýšení funkčních

vlastností textilií. Navíc je použita ultrazvuková akustická metoda in-situ pro vývoj nových multifunkčních nanokompozitů bavlna-TiO<sub>2</sub> (CT).

Ultrazvukovou akustickou metodou byly úspěšně syntetizovány nanočástice oxidu titaničitého (TiO<sub>2</sub>) ve formě čistého anatasu, které mají průměrnou velikost 4 nm a jsou vysoce fotoaktivní. Za pomoci metody centrálního kompozitního designu (CCD) a metody povrchové odezvy (RSM) byl zkoumán vliv procesních proměnných (koncentrace prekurzorů a doba sonizace) na výsledný produkt. Vlastnosti připravených nanočástic (RNP) byly analyzovány skenovací elektronovou mikroskopií (SEM), dynamickým rozptylem světla (DLS), transmisní elektronovou mikroskopií (TEM), rentgenovou difraktoметриí (XRD) a Ramanovou spektroskopií. V experimentech ověřujících fotokatalytické vlastnosti byla použita metylenová modř (MB), která je považována za model organické znečišťující látky v textilním průmyslu. Pro posouzení fotokatalytických vlastností (účinnost v odstraňování barviva) byla provedena srovnávací analýza vyvinutého fotokatalyzátoru s komerčně dostupným fotokatalyzátorem Degussa P25. Rychlé odstranění MB v případě RNP naznačuje jejich vyšší fotokatalytickou aktivitu než P25. Za optimálních podmínek (10ml titanium tetraisopropoxidu (TTIP), 4ml etylenglykolu (EG) konc. a doba sonizace 1 h) byla dosažena maximální účinnost odstraňování barviva 99%. Je zajímavé, že při kalcinaci nebyl nalezen žádný významný rozdíl ve fotokatalytickém výkonu RNP. Samočisticí účinnost RNP aplikovaných na bavlnu byla navíc vyhodnocena v barevném prostoru RGB. Získané výsledky ukazují na významný vliv ultrazvukového působení na fotokatalytický výkon čistého anatasu než na jakýkoli jiný hybridní typ nanočástic oxidu titaničitého.

V dalším experimentu bylo dosaženo povrchové fixace RNP na bavlněnou tkaninu ultrafialovým zářením (UV). Adheze nanočástic na povrchu vlákna, tahové chování a fyzikálně chemické změny před UV ozářením a po něm, byly zkoumány pomocí spektrometrů SEM, Energy Dispersive X-ray (EDX) a spektroskopií s induktivní dvojitou plazmovou atomovou emisí (ICP-AES). Experimentální proměnné, tj. množství nanočástic TiO<sub>2</sub>, teplota systému a doba UV záření byly optimalizovány pomocí CCD a RSM. Také byly vyvinuty dva matematické modely pro aplikaci TiO<sub>2</sub> na bavlnu a pevnost v tahu bavlny po UV ozáření. Modely byly dále použity k potvrzení získaných výsledků. Byla vyrobena samočisticí tkanina synergickou kombinací bavlny s vysoce fotoaktivními nanočásticemi TiO<sub>2</sub>. Byla hodnocena stabilita při UV záření a samočisticí vlastnosti vyrobené tkaniny.

Nakonec byly ultrazvukovou akustickou metodou in situ připraveny nanokompozity bavlna-TiO<sub>2</sub> (CT) s multifunkčními vlastnostmi. Působení ultrazvuku bylo použito jako potenciální nástroj pro vývoj CT nanokompozitů při nízké teplotě v přítomnosti tetrachloridu titaničitého (TTC) a isopropanolu (ISP). Syntetizované vzorky byly charakterizovány metodami XRD, SEM, EDX a ICP-AES. Dále byly sledovány funkční vlastnosti jako ultrafialový ochranný faktor (UPF), samočisticí schopnosti, stálost v praní, antimikrobiální vlastnosti a pevnost CT nanokompozitů v tahu. Pro vyhodnocení vybraných vlivů byly využity metody CCD a RSM. Výsledky potvrzují současně vznik a inkorporaci anatasového TiO<sub>2</sub> s průměrnou velikostí krystalů 4 nm na bavlněnou tkaninu, vzniká materiál s vynikajícími fotokatalytickými vlastnostmi. Samočisticí účinnost CT nanokompozitů i po 30 cyklech praní naznačuje jejich vynikající životnost. Při statistické analýze vybraných proměnných v přípravě a fixaci TiO<sub>2</sub> na bavlnu byly ověřeny jejich významné účinky na fotokatalytické vlastnosti CT nanokompozitů.

#### **Klíčová slova**

TiO<sub>2</sub>; Anatas; Fotokatalýza; Sonochemická syntéza; Degradace barviv; Ultrazvukové ozařování; Etylenglykol; Odpovídající povrchy; Samostabilizace; Samočištění; Nanočástice; Ultrazvukové akustické metody; Faktor ochrany proti ultrafialovému záření; Nanokompozity

<b>Contents</b>	
<b>Abstract</b> .....	<b>3</b>
<b>Abstrakt</b> .....	<b>3</b>
<b>Contents</b> .....	<b>5</b>
<b>1 Introduction</b> .....	<b>7</b>
<b>1.1 Problem statement</b> .....	<b>7</b>
<b>2 Purpose and aim of the thesis</b> .....	<b>7</b>
<b>3 Overview of the current state of problem</b> .....	<b>8</b>
<b>4 Methods used, studied material</b> .....	<b>8</b>
<b>4.1 Experiments for the synthesis of TiO<sub>2</sub> NPs (RNP)</b> .....	<b>8</b>
4.1.1 Materials for the synthesis of TiO <sub>2</sub> NPs .....	9
4.1.2 Design of experiment for the synthesis of TiO <sub>2</sub> NPs.....	9
4.1.3 Methodology for the synthesis of TiO <sub>2</sub> NPs.....	10
4.1.4 Characterization of Resulting Nanoparticles (RNP).....	10
4.1.5 Photocatalytic performance of RNP .....	10
<b>4.2 Experiments for the stabilization of TiO<sub>2</sub> NPs onto cotton</b> .....	<b>11</b>
4.2.1 Materials for the stabilization of TiO <sub>2</sub> NPs onto cotton .....	11
4.2.2 Design of experiment for the stabilization of TiO <sub>2</sub> NPs onto cotton.....	11
4.2.3 Suspension and deposition of TiO <sub>2</sub> NPs onto cotton.....	11
4.2.4 Stabilization of TiO <sub>2</sub> NPs onto cotton through UV light.....	11
4.2.5 Characterization of the developed samples.....	11
4.2.6 Durability of stabilized TiO <sub>2</sub> NPs against leaching .....	11
4.2.7 Self-cleaning efficiency of the stabilized TiO <sub>2</sub> NPs after UV irradiations .....	11
<b>4.3 Experiments for In-situ development of multifunctional Cotton-TiO<sub>2</sub> (CT) nanocomposites</b> ...	<b>12</b>
4.3.1 Materials for multifunctional CT nanocomposites .....	12
4.3.2 In-situ synthesis and deposition of TiO <sub>2</sub> NPs on cotton .....	12
4.3.3 Design of experiment for the development of CT nanocomposites.....	12
4.3.4 Characterization of CT nanocomposites .....	12
4.3.5 UPF efficiency of CT nanocomposites .....	12
4.3.6 Self-cleaning efficiency of CT nanocomposites .....	13
4.3.7 Antimicrobial efficiency of CT nanocomposites .....	13
4.3.8 Washing durability of CT nanocomposites.....	13
4.3.9 Tensile strength of CT nanocomposites.....	13
<b>5 Summary of the results achieved</b> .....	<b>13</b>
<b>5.1 Results and discussions for the synthesis of TiO<sub>2</sub> NPs</b> .....	<b>14</b>
5.1.1 Characterization of Resulting Nanoparticles (RNP).....	14
5.1.2 Optimization of experimental variables for RNP.....	15
5.1.3 Photocatalytic evaluation of RNP .....	15
<b>5.2 Results and discussions for stabilization of TiO<sub>2</sub> NPs onto cotton</b> .....	<b>16</b>

5.2.1	SEM analysis and EDX spectra of TiO <sub>2</sub> NPs stabilized by UV irradiations .....	16
5.2.2	ICP-AES analysis of TiO <sub>2</sub> NPs stabilized by UV irradiations .....	18
5.2.3	Leaching durability .....	18
5.2.4	Self-cleaning efficiency of TiO <sub>2</sub> NPs stabilized by UV irradiations .....	19
5.2.5	Statistical analysis of TiO <sub>2</sub> NPs stabilized by UV irradiations.....	19
<b>5.3</b>	<b>Results and discussions for In-situ developed multifunctional CT nanocomposites .....</b>	<b>22</b>
5.3.1	SEM images and EDX spectra.....	22
5.3.2	XRD analysis .....	23
5.3.3	ICP-AES elemental analysis .....	24
5.3.4	In-situ synthesis and deposition of TiO <sub>2</sub> NPs on cotton .....	24
5.3.5	UPF efficiency of CT nanocomposites .....	25
5.3.6	Self-cleaning efficiency of CT nanocomposites .....	25
5.3.7	Antimicrobial efficiency of CT nanocomposites .....	25
5.3.8	Washing durability of CT nanocomposites.....	25
5.3.9	Tensile strength of CT nanocomposites.....	26
5.3.10	Statistical analysis of CT nanocomposites .....	26
5.3.11	Reusability and sequential application of CT nanocomposites .....	28
<b>6</b>	<b><i>Evaluation of the results and new findings .....</i></b>	<b>33</b>
6.1	<b>Conclusion.....</b>	<b>33</b>
6.2	<b>Follow-up work .....</b>	<b>34</b>
<b>7</b>	<b><i>References .....</i></b>	<b>34</b>
<b>8</b>	<b><i>List of papers published by the author.....</i></b>	<b>37</b>
8.1	<b>Publications in impact factor journals .....</b>	<b>37</b>
8.2	<b>Contributions in international conferences .....</b>	<b>37</b>
8.3	<b>Book chapters .....</b>	<b>37</b>
8.4	<b>Citations .....</b>	<b>38</b>
	<b><i>Resume .....</i></b>	<b>39</b>

## **1 Introduction**

Nano Science or Nanotechnology (NST) manipulates matter on nanoscale by keeping at least one dimension less than 100 nm to develop products with extremely novel properties and functions. NST has gained much attention in recent years due to its fundamentals i.e. surface area to volume ratio and quantum confinement effect [1; 2]. Advances in NST have shown tremendous impact in the field of pharmaceuticals, materials science, energy, electronics and textiles [3-10]. Researchers are successfully using numerous kinds of NMs in textile industry [11-18]. TiO<sub>2</sub> is the most significant and effective material which has been extensively employed in this field. The most significant reasons of its use in multiple applications are high photocatalytic activity, non-toxicity and chemical stability. The role of anatase TiO<sub>2</sub> as a photocatalyst in self-cleaning and self-sterilizing coatings, photo degradation of organic toxins, gas sensors, biomedicines, energy, air and water purification are of great importance [19-22]. Sonochemical synthesis is a promising route that enhances physical and chemical properties of a material through acoustic cavitation i.e. rapid formation, growth and collapse of unstable bubbles. The key advantages of using this method are its simplicity and energy efficiency. This method has been efficiently used as an outstanding tool for low temperature synthesis of nanocrystalline TiO<sub>2</sub> [23; 24].

### **1.1 Problem statement**

In textiles, the stabilization of NMs has been introduced during the last decade. Cheng et al. reported that there is almost no attraction between textile substrates (polymeric materials) and metal oxides particles (inorganic materials). This happens due to the difference in surface energy of the two above mentioned materials that produces repellence on their interfaces [25]. So, the stabilization of NPs on textiles is not permanent particularly against washing. Regardless of the above-mentioned dilemma, researchers continued their efforts and used different approaches to embed or stabilize TiO<sub>2</sub> NPs on the surface of textiles [26-28].

## **2 Purpose and aim of the thesis**

The primary aims and overall objectives of this dissertation are:

- ❖ Synthesize TiO<sub>2</sub> Nanoparticles (NPs) in anatase form by Ultrasonic Acoustic Method (UAM) with novel reagents and incorporate them on textiles by two different approaches i.e. dip-pad-dry and UV induced stabilization and further utilised them as an efficient photocatalyst in multiple applications such as dyes degradation, self-cleaning, UV protecting clothes and antimicrobial finishes etc.
- ❖ Comparison of the developed photocatalyst with commercially available photocatalyst named Degussa P25 for higher photocatalytic efficiency.
- ❖ In-situ fabrication of Cotton-TiO<sub>2</sub> (CT) nanocomposites through UAM by using TiCl<sub>4</sub> or titanium tetrachloride (TTC) as a novel reagent.
- ❖ Analyse the role of ultrasonic irradiations and TiO<sub>2</sub> on the surface and structural properties of CT nanocomposites.
- ❖ Improve the characterization of pristine cotton by incorporation ultrafine TiO<sub>2</sub> NPs onto cotton.
- ❖ A comparative analysis of the developed method with conventional method explains the benefits of novel Ultrasonic Acoustic Method in textiles and composites industries.
  
- ❖ Durability of successfully deposited TiO<sub>2</sub> NPs on cotton fabric is evaluated against washing to investigate the colouring effect of applied materials on fabric.
- ❖ Optimization of the process variables by Central Composite Design (CCD) and Response Surface Methodology (RSM) to obtain more precise and accurate results.
- ❖ Analysis of the obtained results through regression and quadratic functions enhances the significance of the experiments and the development of mathematical models to predict the responses at any given point.
- ❖ Evaluation and increment in the efficiency of the functional properties i.e. Ultraviolet Protection Factor (UPF), dyes degradation efficiency, tensile strength etc., of the developed CT nanocomposites for their efficient use in different applications.

### ***3 Overview of the current state of problem***

This Chapter enlightens the experimental investigations relevant to this dissertation that is divided into two main sections. The first section provides a comprehensive information about the synthesis mechanisms, experimental conditions, relevant parameters, used reagents and the relevant literature regarding synthesis methods mostly used in the fabrication of TiO<sub>2</sub> nanoparticles (NPs) while the applications are in the second section.

Ethylene Glycol (EG) has been extensively used in the synthesis of metal oxide nanomaterials (NMs) as it has strong reducing power and high boiling point [29; 30]. Many researchers have utilized EG in the synthesis of metal oxides by developing glycolated precursors because of its ability to coordinate with transition metal ions [31; 32]. Abidi et al. reported sol-gel stabilization of TiO<sub>2</sub> on cotton fabric that improves UV scattering properties of cotton. They further used curing process to stabilize the developed nanosol on cotton [33]. Perelshtein et al. reported an ultrasonic assisted stabilization of TiO<sub>2</sub> NPs on cotton fabric to impart antimicrobial properties. Their results revealed that TiO<sub>2</sub> in its anatase and rutile form provides significant antimicrobial effects against microorganisms [34].

Gashti and Almasian reported the stabilization of carbon nanotubes on cotton fabric by UV radiations in order to develop flame retardant carbon/cellulose composites coatings [35]. In another study, Gashti et al. reported the incorporation of silica/kaolinite network on cotton surface through UV irradiations using succinic acid as a cross-linking agent to create a thermal resistant hydrophobic surface for cellulose based textiles [36].

Huang et al. utilized titanium tetraisopropoxide (TTIP) and titanium tetrachloride (TTC) as titanium sources to synthesize anatase and rutile phase of TiO<sub>2</sub> through sonication process respectively [37]. Guo et al. harnessed high intensity ultrasonic waves for the synthesis of TiO<sub>2</sub> NPs at 90 °C and explained that ultrasonic waves can use as an efficient tool for low temperature synthesis of nanocrystalline TiO<sub>2</sub> [38]. Ghows and Enterazi used low intensity ultrasonic waves at low temperature for the synthesis of TiO<sub>2</sub> NPs by the hydrolysis of titanium precursor [39].

During the last decade, the immobilization of NPs on textile substrates have been investigated by different methods but a few dealt with an in-situ Ultrasonic Acoustic Method (UAM). This method is useful to enhance washing durability and finishing processes but regardless of the benefits of UAM, sol-gel method is used mostly for the synthesis and deposition of NPs on textile substrates. With sol-gel method, Uddin et al. deposited TiO<sub>2</sub> NPs on cotton fabric at low temperature which induced UV protecting and self-cleaning properties to cotton fabric [40]. The first section of this dissertation represents the unique demonstration that metal alkoxide such as TTIP interact with EG under ultrasonic irradiations and synthesize pure anatase form of TiO<sub>2</sub> NPs with smaller size and higher crystallinity that enhances the photocatalytic performance of the developed photocatalyst. In addition to the precursors discussed here, it is believed that this approach is a generic one and can be extendable for other titanium precursors and synthesis routes. The stabilization of TiO<sub>2</sub> NPs on cotton by UV light is investigated in the second section.

An in-situ method for the development of cotton-TiO<sub>2</sub> (CT) nanocomposites is presented in the last section. Ultrasonic homogenizer was utilized for simultaneous synthesis and deposition of anatase TiO<sub>2</sub> on cotton fabric for multifunctional properties and applications. This study was conducted to investigate the synergistic role of sono synthesized TiO<sub>2</sub> NPs on cotton fabric and to explain the influence of ultrasonic irradiations on photocatalytic, UV protection, self-cleaning, antimicrobial and tensile properties of the CT nanocomposites. The variables i.e. concentrations of Titanium Tetrachloride (TTC) and Isopropanol (ISP), and ultrasonic irradiations time, were optimized accurately by Central Composite Design (CCD) to achieve the optimal conditions and functional properties.

### ***4 Methods used, studied material***

This Chapter consists the materials and methodology for the synthesis of TiO<sub>2</sub> NPs (RNP) as an efficient photocatalyst than Degussa P25; the incorporation or stabilization of RNP onto cotton by UV light irradiations; and an in-situ development of multifunctional Cotton-TiO<sub>2</sub> (CT) nanocomposites that has been divided into three sections respectively.

#### ***4.1 Experiments for the synthesis of TiO<sub>2</sub> NPs (RNP)***

This section explains the experimental part for the synthesis of TiO<sub>2</sub> NPs (RNP) in pure anatase form and the characterization techniques used in this study.



#### 4.1.1 Materials for the synthesis of TiO<sub>2</sub> NPs

Titanium Tetraisopropoxide (TTIP) with chemical formula  $Ti(OC_3H_7)_4$ , Ethylene Glycol (EG) with chemical formula  $HOCH_2CH_2OH$ , Methylene Blue (MB) dye with chemical formula  $C_{16}H_{18}ClN_3S$  and Ethanol with chemical formula  $C_2H_5OH$  were received from Sigma-Aldrich. Commercially available photocatalyst named P25 (99.9 %) composed of 80 % anatase and 20 % rutile with specific surface area  $59\ m^2\ g^{-1}$  and average particle size  $18\ nm$  was received from Degussa corporation. 100 % pure Plain weave cotton fabric with fabric mass  $115\ gm^{-2}$  was received from Department of Material Engineering, Technical University of Liberec, Czech Republic. All reagents were of analytical standard and used as received.

#### 4.1.2 Design of experiment for the synthesis of TiO<sub>2</sub> NPs

A Central Composite Design (CCD) is a set of experimental design with three different design points i.e. factorial points ( $\pm 1$ ), centre point (0) and star/axial points ( $\pm\alpha$ ) which is beneficial in Response Surface Methodology (RSM) to fit a quadratic model in order to estimate the effect of curvature or to find out the maximum and minimum of a variable. In CCD, the centre point is replicated for getting more precision of the experiment. The general form of a CCD with three input variables/factors (A, B, C) and their coded values ( $\pm 1$ ), centre point (0) and axial/star points ( $\pm\alpha$ ) is illustrated in Figure 4-1. For 3 factors CCD, the value of  $\alpha$  is 1.68.

Table 4-1 shows the input variables (factors) with their coded values (minimum, maximum) and their central points whereas Table 4-2 illustrates the factors level setting in their coded form based on CCD.

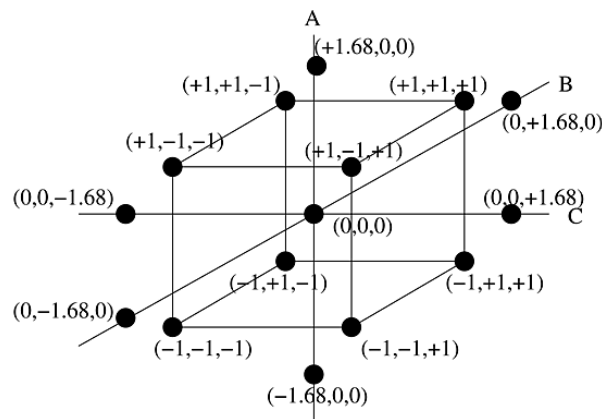


Figure 4-1 General form of a three factors central composite design with coded values.

Table 4-1 The 3-factors CCD matrix for experimental variables with coded values for the synthesis of TiO<sub>2</sub> NPs

Factor	Name	Unit	Coded Values	Central Point	Mean	Std. Dev.
A	TTIP	mL	-1=4    1=8	6	6	1.8
B	EG	mL	-1=3    1=5	4	4	0.9
C	Sonication Time	h	-1=1    1=3	2	2	0.8

Design-Expert version 10 by Stat-Ease corporation was used for statistical analysis throughout the experiments. The influence of variables on the results including:  $Y = \text{MB removal } [\%]$  was adjusted by using a quadratic Equation 1:

$$Y = b_0 + \sum b_i X_i + \sum b_{i,j} X_i X_j + \sum b_{i,i} X_i^2 \quad i \geq j \quad i, j = 1, 2, 3 \quad [1]$$

Where  $b_0$  is the coefficient of constant term,  $b_i$  represents the coefficient of linear term that explains the persuade of the variables,  $b_{ii}$  is the coefficient of quadratic term and  $b_{ij}$  represents the coefficient of two factors interaction [24; 41].

#### 4.1.3 Methodology for the synthesis of TiO<sub>2</sub> NPs

In the experimental part, liquid TTIP was added drop by drop into a beaker containing 50 mL ethanol with simultaneous addition of EG into the running solution with TTIP:EG ratio 2:1 under continuous magnetic stirring at 500 rpm. The temperature of the solution was adjusted to 80 °C by using the hot plate equipped with magnetic stirrer. The solution was then sonicated for different time intervals based on CCD under ultrasonic homogeniser system (Bandelin Sonopuls HD 3200, 20 kHz, 200 W, 50 % efficiency) to complete the reaction mechanism. The resulting white flocculates were washed several times with ethanol to remove impurities. The white flocculates were then centrifuged at 6000 rpm for 5 min to separate solid particles. The centrifuged solid was dried at 100 °C for 2 h in an oven and then further characterized. In order to emphasize the fundamental influence of ultrasonic irradiations, similar sample was developed by conventional magnetic stirring method.

*Table 4-2 The 3-factors general CCD matrix for experimental variables with coded values and factors level setting for the synthesis of TiO<sub>2</sub> NPs*

Experimental Trial	Factors Level Setting		
	A	B	C
1	-1	-1	-1
2	1	-1	-1
3	-1	1	-1
4	1	1	-1
5	-1	-1	1
6	1	-1	1
7	-1	1	1
8	1	1	1
9	-α	0	0
10	α	0	0
11	0	-α	0
12	0	α	0
13	0	0	-α
14	0	0	α
15	0	0	0
16	0	0	0
17	0	0	0
18	0	0	0
19	0	0	0
20	0	0	0

#### 4.1.4 Characterization of Resulting Nanoparticles (RNP)

Scanning Electron Microscopic (SEM), Transmission Electron Microscopy (TEM), Powder X-ray Diffraction (XRD) were used to characterize the developed samples. The size of the crystals was calculated through the line broadening of the plane reflection by Scherer's crystallite equation as presented in Equation 2:

$$D = \frac{K\lambda}{\beta \cos\theta} \quad [2]$$

Where  $D$  represents the crystallite size and  $\lambda$  is the wavelength of the X-ray radiations.

#### 4.1.5 Photocatalytic performance of RNP

The photocatalytic performance of RNP and P25 was studied by decolouration of MB solution under UV irradiations. The colour removal efficiency (CR%) was calculated by Equation 3:

$$CR\% = \left[ \frac{C_o - C}{C_o} \right] \times 100 \quad [3]$$

Where  $C_o$  and  $C$  represents the initial and final concentration of MB in the solution, respectively.

## 4.2 Experiments for the stabilization of TiO<sub>2</sub> NPs onto cotton

This section explains the experimental part for the stabilization of TiO<sub>2</sub> NPs (RNP) onto cotton fabric by UV light irradiations and the characterization techniques used in this study.

### 4.2.1 Materials for the stabilization of TiO<sub>2</sub> NPs onto cotton

100 % pure cotton fabric (plain weave with fabric mass 115 gm<sup>-2</sup>) was used. TiO<sub>2</sub> NPs with average particle size 4 nm and specific surface area 150 m<sup>2</sup>g<sup>-1</sup> were used in this study as synthesized and reported in our up given investigation [42]. Distilled water was used throughout the study.

### 4.2.2 Design of experiment for the stabilization of TiO<sub>2</sub> NPs onto cotton

The experimental design for the stabilization of TiO<sub>2</sub> NPs onto cotton is based on CCD. The general form of CCD is discussed in detail in the section 4.1.2. The input variables (factors) with their coded values (minimum, maximum) and central points for the stabilization of TiO<sub>2</sub> NPs onto cotton are given in *Table 4-3*.

*Table 4-3 The 3-factors CCD matrix for experimental variables with coded values for the stabilization of TiO<sub>2</sub> NPs onto cotton*

Factor	Name	Unit	Coded Values		Central Point	Mean	Std. Dev.
A	TiO <sub>2</sub> Dosage	gL <sup>-1</sup>	-1=4	1=8	6	6	1.8
B	Temperature	°C	-1=30	1=60	45	45	12.6
C	UV Irradiation Time	min	-1=40	1=120	80	80	33.9

### 4.2.3 Suspension and deposition of TiO<sub>2</sub> NPs onto cotton

A suspension of TiO<sub>2</sub> NPs with distilled water was developed by ultrasonic homogeniser. The concentration of TiO<sub>2</sub> NPs varying from 2 gL<sup>-1</sup> to 10 gL<sup>-1</sup> according to CCD. Dip-pad-dry method was used to embed TiO<sub>2</sub> NPs onto cotton fabric.

### 4.2.4 Stabilization of TiO<sub>2</sub> NPs onto cotton through UV light

To investigate the adhesion, incorporation and surface changes, all TiO<sub>2</sub> treated and untreated samples were irradiated under UV light for different time intervals ranging from 15 min to 150 min according to CCD.

### 4.2.5 Characterization of the developed samples

The morphological changes on the surface of TiO<sub>2</sub> treated samples, untreated samples and samples 1-20, were observed by UHR-SEM Zeiss Ultra Plus with an Energy Dispersive X-ray (EDX) Spectrometer Oxford X-max 20. The incorporated amount of TiO<sub>2</sub> NPs on cotton surface after UV irradiations was estimated by Inductive Couple Plasma-Atomic Emission Spectroscopy (ICP-AES) elemental analysis.

### 4.2.6 Durability of stabilized TiO<sub>2</sub> NPs against leaching

The durability of embedded TiO<sub>2</sub> NPs onto cotton fabric against washing was evaluated according to ISO 105 C06 (B1M) standard test method. For leaching, the amount of Ti<sup>+4</sup> ions presented in the leaching solution was estimated to evaluate the adhesion and stability of the developed samples. For this purpose, different samples were treated with 1M NaCl solution at laboratory conditions for 6 h.

### 4.2.7 Self-cleaning efficiency of the stabilized TiO<sub>2</sub> NPs after UV irradiations

Self-cleaning efficiency was evaluated on the basis of degradation activity of coffee stain under daylight irradiations for 12 h. The study was conducted by taking swatches (4x4 cm) from all samples and a coffee stain was dropped vertically on them. After that, all samples were dried and exposed to daylight irradiations for different time intervals and colour difference was estimated according to *Equation 4*:

$$\Delta E = [\Delta L^2 + \Delta a^2 + \Delta b^2]^{1/2} \quad [4]$$

Where  $L$  refers to lightness of the fabric,  $a$  and  $b$  stand for red-green colour and yellow-blue colour respectively.

### 4.3 Experiments for In-situ development of multifunctional Cotton-TiO<sub>2</sub> (CT) nanocomposites

This section explains the experimental part for the development of multifunctional CT nanocomposites and the characterization techniques used in this study.

#### 4.3.1 Materials for multifunctional CT nanocomposites

100 % pure plain cotton fabric with mass  $115 \text{ gm}^{-2}$  was used. Titanium Tetrachloride (TTC) with chemical formula  $\text{TiCl}_4$ , Isopropanol (ISP) with chemical formula  $(\text{CH}_3)_2\text{CHOH}$  and Methylene Blue (MB) with chemical formula  $\text{C}_{16}\text{H}_{18}\text{ClN}_3\text{S}$  were received from Sigma Aldrich.

#### 4.3.2 In-situ synthesis and deposition of TiO<sub>2</sub> NPs on cotton

TiO<sub>2</sub> nanocrystalline particles with smaller size have been simultaneously synthesized and deposited on cotton surface by Ultrasonic Acoustic Method (UAM). Cotton fabric was immersed in a vessel containing TTC, ISP and water under ultrasonic system (Bandelin Sonopuls HD 3200, 20 kHz, 200 W, 50 % efficiency) to complete the reaction mechanism. The effective power of ultrasonic waves emitted in the solution was  $100 \text{ Wcm}^{-2}$  experimentally determined by calorimetric measurement. The detailed mechanism for the development of Cotton-TiO<sub>2</sub> (CT) nanocomposites is described in [Figure 4-2](#). In this unique study, varying amount of ISP (0.5-8 mL) was dissolved in 100 mL of distilled H<sub>2</sub>O by v/v percentage under continuous stirring in order to make homogeneous solution. A squared cotton fabric sample (12x12 cm) was then immersed in the solution for 2-3 min and then drop by drop addition of TTC into the solution bath. The immersed fabric was then sonicated for different time intervals varying from 0.25 h to 4 h. The treated samples were dried in oven for 2 h at 70 °C. To find out the crucial role to ultrasonic irradiations, conventional magnetic stirring was used to prepare similar sample that 10 mL TTC, 6 mL ISP and cotton fabric (12x12 cm) at 70 °C were magnetically stirred at 500 rpm. This sample was named as sample C.

#### 4.3.3 Design of experiment for the development of CT nanocomposites

The experimental design for the development of CT nanocomposites is based on CCD. The general form of CCD is discussed in detail in the section 4.1.2. The input variables (factors) with their coded values (minimum, maximum) and central points for the development of CT nanocomposites are given in [Table 4-4](#).

**Table 4-4** The 3-factors CCD matrix for experimental variables with coded values for the development of CT nanocomposites

Factor	Name	Unit	Coded Values		Central Point	Mean	Std. Dev.
A	TTC	mL	-1=4	1=8	6	6	1.8
B	ISP	mL	-1=2	1=6	4	4	1.7
C	Sonication Time	h	-1=1	1=3	2	2	0.8

#### 4.3.4 Characterization of CT nanocomposites

The morphological changes on the surface of cotton fabric after in-situ deposition of TiO<sub>2</sub> NPs were observed by UHR-SEM Zeiss Ultra Plus with an accelerating voltage 2 kV equipped with an Energy Dispersive X-ray (EDX) Spectrometer Oxford X-max 20. XRD patterns were collected by X'Pert PRO X-ray Diffractometer. The observed patterns were analysed and compared with standard patterns of JCPDS card no. (21-1272). The crystallite size was calculated through [Equation 2](#).

#### 4.3.5 UPF efficiency of CT nanocomposites

In order to determine the Ultraviolet Protection Factor (UPF) of the developed CT nanocomposites, measurements were conducted according to AS/NZS 4399:1996 with a Varian Cary 500 UV-Vis-NIR Spectrophotometer with integrated sphere. For each sample, four measurements were performed with different directions and the average of all four scans was taken as a final UPF value which was calculated by [Equation 5](#).

$$UPF = \frac{\sum_{280}^{400} S_{\lambda} E_{\lambda} \Delta_{\lambda}}{\sum_{280}^{400} S_{\lambda} E_{\lambda} T_{\lambda} \Delta_{\lambda}} \quad [5]$$

In Equation 5,  $S_{\lambda}$  is the solar spectral irradiance,  $E_{\lambda}$  is the relative erythral spectral response,  $T_{\lambda}$  is the average spectral transmittance of the sample and  $\Delta_{\lambda}$  is the measured wavelength interval in nanometres.

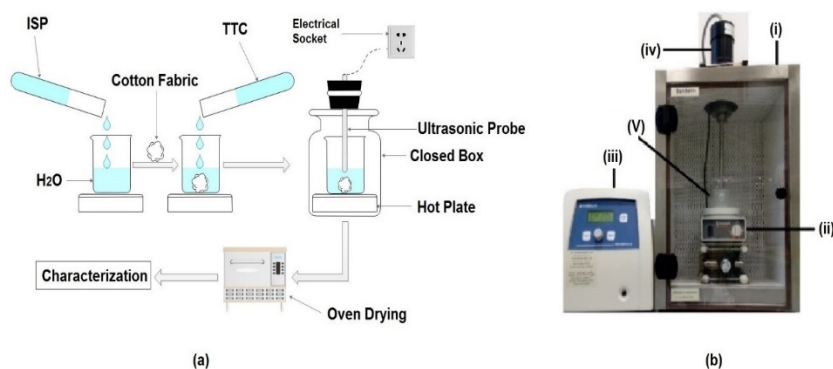


Figure 4-2 (a) Schematic representation for the development of CT nanocomposites; (b) Experimental Setup: (i) closed box (ii) hot plate (iii) ultrasonic wave generator (iv) ultrasonic probe (v) immersed fabric sample.

#### 4.3.6 Self-cleaning efficiency of CT nanocomposites

Self-cleaning efficiency of the developed CT nanocomposites was evaluated on the basis of colour change and degradation activity of MB stain under daylight irradiations for 24 h. All samples were dried in air and then exposed to daylight irradiations for different time intervals and colour change was estimated according to Equation 6.

$$\Delta RGB = [\Delta R^2 + \Delta B^2 + \Delta G^2]^{1/2} \quad [6]$$

#### 4.3.7 Antimicrobial efficiency of CT nanocomposites

The quantitative antimicrobial efficiency of the developed CT nanocomposites was evaluated against Staphylococcus aureus (S. aureus) and Escherichia coli (E. coli) microorganisms according to AATCC test method 100-2012.

#### 4.3.8 Washing durability of CT nanocomposites

Finishing applications have a colouring effect on fabrics so the durability of TiO<sub>2</sub> NPs synthesized by an in-situ UAM on cotton fabric against washing was evaluated according to ISO 105 C06 (B1M). According to the standard test method, each washing cycle completed with 4 gL<sup>-1</sup> detergent at 50 °C for 45 min time interval is equal to five home launderings [15]. The washed specimen was then rinsed and dried at 60 °C for 15 min after each washing cycle. A Varian Cary 500 UV-Vis-NIR Spectrophotometer was used to evaluate absorption spectra of washing effluents.

#### 4.3.9 Tensile strength of CT nanocomposites

Tensile strength of the developed CT nanocomposites was tested on TIRA Test 2300 with Constant Rate of Extension (CRE) according to standard test method ISO 13934-1.

## 5 Summary of the results achieved

This Chapter explains the results for the synthesis of TiO<sub>2</sub> NPs (RNP); the stabilization of RNP onto cotton by UV light irradiations and an in-situ development of multifunctional Cotton-TiO<sub>2</sub> (CT) nanocomposites in three sections respectively.

## 5.1 Results and discussions for the synthesis of TiO<sub>2</sub> NPs

This section explains the results for the synthesis of TiO<sub>2</sub> NPs (RNP) and discusses their applications in details.

### 5.1.1 Characterization of Resulting Nanoparticles (RNP)

In *Figure 5-1*, the results of the SEM analysis are illustrated which indicate that Resulting Nanoparticles (RNP) are more spherical in shape than P25. The size of RNP is much smaller in comparison to P25 as observed in *Figure 5-1*. The average particle size for P25 and RNP were 18 nm and 4 nm respectively confirmed by particle size distribution as presented in *Figure 5-2*.

TEM analysis of RNP and P25 is described in *Figure 5-3*. The TEM results indicate that the RNP are more spherical in shape with uniform distribution of particles. Moreover, most of the RNP are separated from each other while agglomeration observed in P25. The inset showed a distinct diffraction rings for RNP corresponding to the crystalline phase while for P25, dull fringes and agglomeration observed. These results indicate that RNP are more crystalline in nature than P25. The ratio of agglomeration in the RNP is insignificant which indicates their good photocatalytic activity as compared to P25. The estimated mean particle size through TEM images is around 4 nm which is in good agreement with XRD results.

The results collected by XRD analysis describe that RNP possessed pure anatase phase with all sharp peaks matched with the standard Powder Diffraction card data base JCPDS (21-1272). In *Figure 5-4*, the highest peak obtained at  $2\theta=25.4^\circ$  represents the (101) plane reflection which is the characteristic peak for pure anatase form of TiO<sub>2</sub> followed by three more primary peaks at  $2\theta=38^\circ$ ,  $48^\circ$  and  $54^\circ$  for (004), (200) and (211) planes respectively. The average crystallite size obtained by using Scherrer's equation is 4 nm. It can be evaluated by the results that RNP have much smaller size as compared to P25. It could be due to EG content into the crystal lattice of RNP that suppress the crystal growth of RNP.

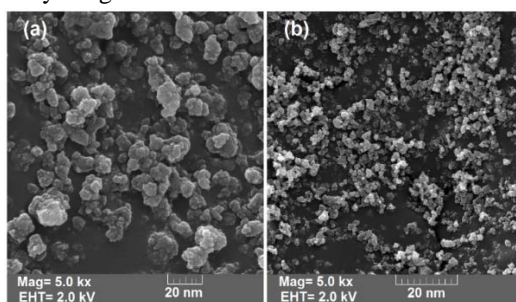


*Figure 5-1 SEM images (a) P25, (b) RNP with optimal conditions TTIP 10 mL, EG 4 mL, Sonication time 1 h.*

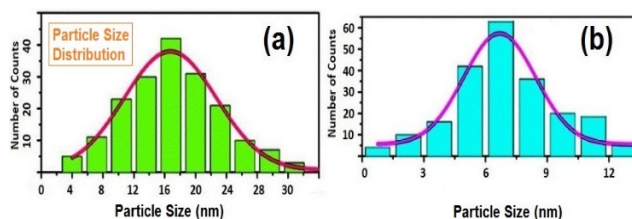


*Figure 5-2 Particle size distribution obtained by DLS (a) P25, (b) RNP with optimal conditions TTIP 10 mL, EG 4 mL, Sonication time 1 h.*



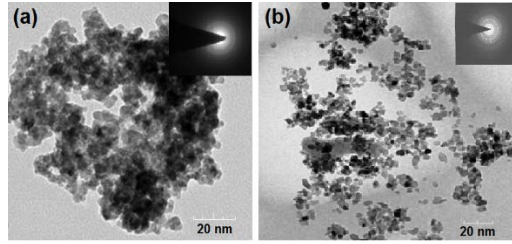


Figure 5-3 TEM images (a) P25, (b) RNP with optimal conditions TTIP 10 mL, EG 4 mL, Sonication time 1 h.

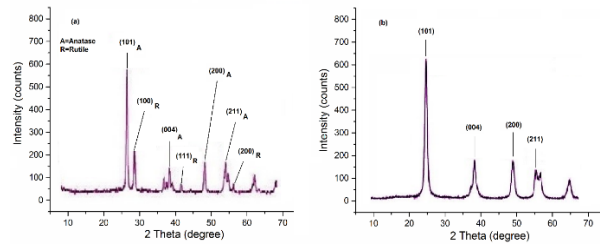


Figure 5-4 XRD pattern (a) P25, (b) RNP with optimal conditions TTIP 10 mL, EG 4 mL, Sonication time 1 h.

### 5.1.2 Optimization of experimental variables for RNP

The design of experiment with different concentrations of TTIP and EG under varying sonication time based on actual values of CCD is presented in *Table 5-1*. Total 20 experimental CCD designed samples were developed as illustrated in *Table 5-1*.

The response surfaces and contour plots were drawn by Design-Expert 10 to evaluate the interactive relationships between the selected variables and MB removal efficiency. The effect of precursor's concentrations and ultrasonic irradiations time on the photocatalytic removal of MB is presented in *Figure 5-5*.

It can be seen in *Table 5-1* that MB removal rate increased from 33 % to 91 %, 33 % to 85 % and 33 % to 91 % by increasing the TTIP and EG concentration and sonication time up to their maximum level. However, the best outcome 99 % was achieved with optimal conditions i.e. TTIP 10 mL, EG 4 mL and sonication time 1 h., whereas, the predicted response value for MB removal at optimal conditions (Sample 4) was 98 %.

MB removal on the basis of developed model is calculated by *Equation 7*:

$$Y = -30.2 + 14.8(TTIP) - 20.5(EG) + 60.9(Time) + 1.0(TTIP * EG) - 2.6(TTIP * Time) - 10.6(EG * Time) - 0.4(TTIP)^2 + 4.4(EG)^2 + 0.3(Time)^2 \quad [7]$$

Analysis of variance (ANOVA) was used to analyse the data for interaction between process variables and responses obtained from samples 1-20 (*Table 5-1*) and results were analysed to judge the goodness of fit. The results indicate that the designed model for MB dye removal is statistically significant for F-value of 273.8 and prob > F of <0.0001 as shown in *Table 5-2*. R-squared coefficient is used to predict the fit of the model.

### 5.1.3 Photocatalytic evaluation of RNP

The photocatalytic activity of RNP and P25 was investigated with 0.5 gL<sup>-1</sup> dose of both photocatalysts by taking initial concentration of MB 50 mgL<sup>-1</sup>. The results illustrated in *Figure 5-6* explain that the decolouration of MB follows decreasing order. It was observed that with the same dosage of RNP, dye solutions have been decoloured within 40 min under UV light while for P25, the dye solutions took longer time to decolour. To confirm the decolouration of MB was due to the presence of RNP and not by the poor light fastness of MB dye, dye solution without photocatalyst was also exposed under UV light. This solution couldn't change its colour

even after longer irradiations time. These results confirm that the higher photo activity of RNP originated due to anatase form induced by ultrasonic irradiations.

## 5.2 Results and discussions for stabilization of TiO<sub>2</sub> NPs onto cotton

This section explains the results for the stabilization of TiO<sub>2</sub> NPs (RNP) onto cotton fabric by UV light irradiations in details for further applications.

### 5.2.1 SEM analysis and EDX spectra of TiO<sub>2</sub> NPs stabilized by UV irradiations

The morphology of developed samples was investigated by SEM and EDX analysis. In *Figure 5-7*, a comparison of pristine cotton (untreated sample) with sample 14 is presented as we obtained highest incorporated amount of TiO<sub>2</sub> NPs for this sample (*Table 5-3*). In *Figure 5-7 (a)*, a clean and smooth surface of pristine cotton can be observed as no treatment was applied on it whereas a huge cluster of TiO<sub>2</sub> NPs deposited as a homogeneous thick layer on the surface of cotton fabric after padding can be seen in *Figure 5-7 (b)*. We also observed that the particles are evenly distributed on the surface of cotton *Figure 5-7 (b)*. In *Figure 5-7 (c)*, it can be seen that after UV irradiations, most of the NPs penetrated inside the cotton fibre structure and the remaining covered the surface as a condense layer and strongly aggregated while a completely rough surface of cotton with sufficient amount of TiO<sub>2</sub> NPs was observed after washing the sample as illustrated in *Figure 5-7 (d)*.

Elemental analysis and detection of existing elements were characterized by EDX spectroscopy. The EDX spectrum of untreated sample and sample 14 are presented in *Figure 5-7 (e-f)* respectively. EDX spectra confirm the existence of TiO<sub>2</sub> NPs on cotton surface. Moreover, higher weight percentage of Ti element in sample 14 indicates higher loading of TiO<sub>2</sub> NPs. These results are in good agreement with SEM results.

**Table 5-1** The 3-factors CCD matrix based on actual values for experimental variables and response, Y=MB Removal, for the synthesis of TiO<sub>2</sub> NPs

Sample	TTIP Conc. [mL]	EG Conc. [mL]	Sonication Time [h]	MB Removal [%] Experimental	MB Removal [%] Predicted
1	6	4	2	67	64
2	6	4	0.25	57	58
3	4	3	1	33	32
4	10	4	1	99	98
5	4	5	3	47	46
6	8	3	1	72	73
7	8	3	3	91	91
8	6	4	2	63	64
9	2	4	2	21	23
10	6	6	2	81	81
11	6	4	2	62	64
12	6	4	2	62	64
13	6	4	2	63	64
14	4	5	1	50	49
15	8	5	3	74	74
16	4	3	3	72	71
17	6	4	4	72	73
18	6	2	2	81	81
19	6	4	2	64	64
20	8	5	2	85	86



**Table 5-2 ANOVA results for MB removal for the synthesis of TiO<sub>2</sub> NPs**

Source	Sum of Squares	df	Mean Square	F Value	p-value Prob > F	Remarks
Model	6536.6	9	726.2	273.8	< 0.0001	Significant
A-TTIP Conc.	4365.6	1	4365.6	1646	< 0.0001	Significant
B-EG Conc.	0.01	1	0.01	0.004	0.9506	Not significant
C-Sonication Time	204.2	1	204.2	77	< 0.0001	Significant
AB	31.7	1	31.7	11.9	0.0061	Significant
AC	243.9	1	243.9	91.9	< 0.0001	Significant
BC	732.5	1	732.5	276.2	< 0.0001	Significant
A <sup>2</sup>	62.6	1	62.6	23.6	0.0007	Significant
B <sup>2</sup>	497.0	1	497	187.4	< 0.0001	Significant
C <sup>2</sup>	2.07	1	2.07	0.78	0.3968	Not significant
Residual	26.5	10	26.5			
Lack of Fit	9.0	5	1.8	0.51	0.7577	Not significant
Pure Error	17.5	5	3.5			
Cor Total	6563.2	19				

R-squared: 0.9960, adjusted R-squared: 0.9923, CV%: 2.47

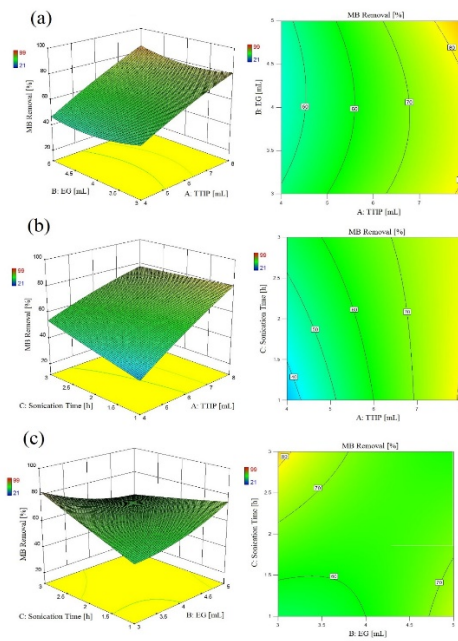


Figure 5-5 The response surfaces and contour plots for photocatalytic dye removal as a function of (a) TTIP conc., EG conc., (b) TTIP conc., Sonication time., (c) EG conc., Sonication time.

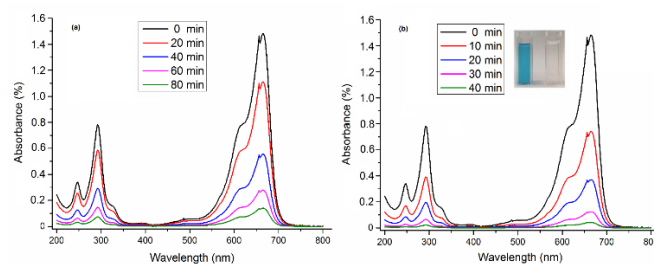


Figure 5-6 UV-Vis spectral changes in MB solution as a function of UV irradiations time. (a) P25, (b) RNP with optimal conditions TTIP 10 mL, EG 4 mL, Sonication time 1 h. The inset shows the digital photograph for colour change of MB before and after treatment.

### 5.2.2 ICP-AES analysis of TiO<sub>2</sub> NPs stabilized by UV irradiations

ICP-AES analysis of samples 1-20 confirmed the presence of TiO<sub>2</sub> NPs on cotton. However, Ti element was not found in untreated sample. In order to estimate the incorporated amount, the characteristic peak of titanium observed in emission spectra was counted and the results were reported in *Table 5-3*. The incorporated amount of TiO<sub>2</sub> NPs for samples 1, 11, 16, 17, 18 were 2123 ppm, 1781 ppm, 2895 ppm, 2999 ppm, 2756 ppm respectively, whereas the highest incorporated amount 3319 ppm was found in sample 14. The results are quite obvious as more dosage of TiO<sub>2</sub> NPs during padding results in more loading on cotton. These results are in good agreement with SEM and EDX results.

### 5.2.3 Leaching durability

The contents of Ti<sup>4+</sup> ions present in the leaching solution were 82 ppm, 107 ppm, 102 ppm, 48 ppm and 39 ppm for sample 3, sample 5, sample 10, sample 14 and sample 18 respectively. These results reveal that only 5 % TiO<sub>2</sub> was removed from the fabric surface by leaching in case of sample 5 whereas this percentage was decreased to 1.4 % for sample 14 and sample 18. On the other side, 63 % TiO<sub>2</sub> was removed for TiO<sub>2</sub> treated sample (without UV treatment). These results indicate that TiO<sub>2</sub> NPs incorporated on cotton surface by UV light irradiations were strongly anchored to the textile substrate as their minimal quantity was withdrawn from the fabric even after 6 h of leaching process.

*Table 5-3 The 3-factors CCD matrix based on actual values for experimental variables and responses, Y<sub>1</sub>= Incorporated amount of TiO<sub>2</sub> NPs after UV irradiations, Y<sub>2</sub>= Tensile strength after UV irradiations, for the stabilization of TiO<sub>2</sub> NPs by UV irradiations*

Sample Name	TiO <sub>2</sub> Dosage [gL <sup>-1</sup> ]	Temperature [°C]	UV Irradiations Time [min]	Y <sub>1</sub> = Incorporated TiO <sub>2</sub> on cotton [ppm]	Y <sub>2</sub> = Tensile Strength [N]
Untreated Sample	0	0	0	0	504
1	6	70	80	2123	482
2	4	30	120	1590	474
3	6	45	80	1383	434
4	6	45	80	1386	426
5	6	45	15	793	465
6	8	30	40	1590	463
7	6	45	80	1380	424
8	4	60	40	898	432
9	6	45	80	1389	427
10	4	30	40	856	498

11	8	60	40	1781	496
12	6	20	80	1763	476
13	2	45	80	759	489
14	8	60	120	3319	490
15	6	45	80	1398	428
16	8	30	120	2895	414
17	10	45	80	2999	492
18	6	45	150	2756	428
19	4	60	120	1805	425
20	6	45	80	1381	420

#### 5.2.4 Self-cleaning efficiency of TiO<sub>2</sub> NPs stabilized by UV irradiations

*Figure 5-8* illustrates that coffee stains were decomposed completely after 12 h of sunlight irradiations through photocatalytic action of TiO<sub>2</sub>. The colour difference was calculated and the results were reported in *Table 5-4*. Significant colour change was observed for samples 1 to 20 as presented in *Figure 5-8*. However, slight colour change was observed for TiO<sub>2</sub> treated sample (without UV treatment) and almost no change in untreated sample even after 12 h of continuous sunlight irradiations. Moreover, the results reveal that more amount of TiO<sub>2</sub> NPs incorporated on the surface of cotton fabric enhances the self-cleaning properties. Higher colour difference leads to better self-cleaning efficiency obtained by sample 14 with optimal conditions as illustrated in *Table 5-3*.

#### 5.2.5 Statistical analysis of TiO<sub>2</sub> NPs stabilized by UV irradiations

The experimental design with different dosage of TiO<sub>2</sub> Nanoparticles (NPs) under varying temperature and UV irradiations time based on actual values of CCD is illustrated in *Table 5-3*. The results include: Y<sub>1</sub>=Incorporated amount of TiO<sub>2</sub> NPs onto cotton after UV irradiations and Y<sub>2</sub>=Tensile strength of cotton after UV irradiations were adjusted by *Equation 1*.

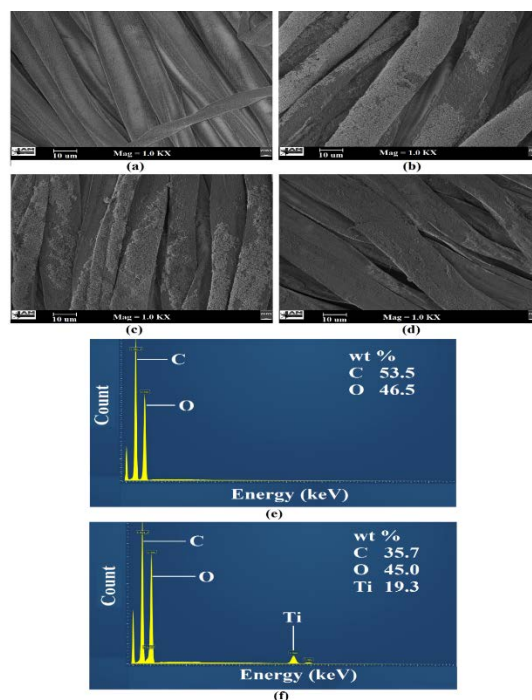


Figure 5-7 SEM analysis of (a) untreated sample, (b) sample 14 before UV treatment, (c) sample 14 after UV treatment, (d) UV treated sample after washing; and EDX spectra of (e) untreated sample (f) sample 14.

**Table 5-4 Self-cleaning efficiency ( $\Delta E$ ) results for the stabilization of  $\text{TiO}_2$  NPs by UV irradiations**

Sample	( $\Delta E$ )	Sample	( $\Delta E$ )
Untreated Sample	4.9	Sample 10	83.9
$\text{TiO}_2$ treated sample (without UV)	48.4	Sample 11	82.6
Sample 1	81.8	Sample 12	83.2
Sample 2	79.6	Sample 13	80.1
Sample 3	80.5	Sample 14	89.7
Sample 4	82.3	Sample 15	83.5
Sample 5	78.4	Sample 16	81.7
Sample 6	79.2	Sample 17	82.6
Sample 7	81.6	Sample 18	83.3
Sample 8	82.8	Sample 19	82.9
Sample 9	80.6	Sample 20	81.8

In *Figure 5-9* and *Figure 5-10*, response surfaces were drawn based on the developed mathematical models for incorporated amount of  $\text{TiO}_2$  NPs and tensile strength respectively. ANOVA results are presented in *Table 5-5* and *Table 5-6*. The results indicate that the designed model for incorporated amount of  $\text{TiO}_2$  NPs on cotton after UV irradiations is statistically significant at F-value 10592.9 and p-value <0.0001 as illustrated in *Table 5-5*. Furthermore, the developed model for tensile strength is significant at F-value 43.1 and p-value <0.0001 as described in *Table 5-6*. R-squared coefficient was used to evaluate the fit of the developed models. The results presented in *Table 5-5* indicate that only 0.01 % of the total variables cannot be explained through this model for incorporated amount of  $\text{TiO}_2$  NPs on cotton after UV irradiations. Furthermore, the results of R-squared for tensile strength indicate that only 2.51 % of the total variables cannot be explained by the model (*Table 5-6*). The incorporated amount of  $\text{TiO}_2$  NPs on cotton after UV irradiations according to the developed model is calculated by *Equation 8*:

$$\begin{aligned}
Y_1 = & 3311.8 - 310.9 \times (\text{Dosage}) - 89.3 \times (\text{Temperature}) - 13.5 \times (\text{UV Time}) + 1.4 \\
& \times (\text{Dosage} \times \text{Temperature}) + 1.8 \times (\text{Dosage} \times \text{UV Time}) + 0.08 \\
& \times (\text{Temperature} \times \text{UV Time}) + 31.0 \times (\text{Dosage})^2 + 0.8 \\
& \times (\text{Temperature})^2 + 0.07 \times (\text{UV Time})^2
\end{aligned}
\tag{8}$$

The tensile strength after UV irradiations according to the developed model is calculated by Equation 9:

$$\begin{aligned}
Y_2 = & 1035.1 - 83.4 \times (\text{Dosage}) - 13.5 \times (\text{Temperature}) - 1.1 \times (\text{UV Time}) + 0.9 \\
& \times (\text{Dosage} \times \text{Temperature}) - 0.03 \times (\text{Dosage} \times \text{UV Time}) + 0.01 \\
& \times (\text{Temperature} \times \text{UV Time}) + 3.8 \times (\text{Dosage})^2 + 0.07 \\
& \times (\text{Temperature})^2 + 3.5 \times (\text{UV Time})^2
\end{aligned}
\tag{9}$$

According to the above regression equations and obtained results (Table 5-3), the optimal points for best possible results are  $8 \text{ gL}^{-1}$   $\text{TiO}_2$  dosage,  $60^\circ \text{C}$  temperature and  $120 \text{ min}$  UV irradiations time. The predicted response values for  $Y_1$  and  $Y_2$  under optimal conditions (Sample 14) are  $3312 \text{ ppm}$  and  $488 \text{ N}$  respectively. The response surfaces are presented in Figure 5-9 and Figure 5-10 for incorporated amount of  $\text{TiO}_2$  NPs on cotton after UV irradiations and tensile strength after UV irradiations respectively. It can be seen in Figure 5-9 and Figure 5-10 that increasing  $\text{TiO}_2$  NPs dosage in the suspension results in more incorporated amount of  $\text{TiO}_2$  NPs on the surface of cotton. Moreover, prolonged UV irradiations time leads to a higher fixation of  $\text{TiO}_2$  NPs on cotton.

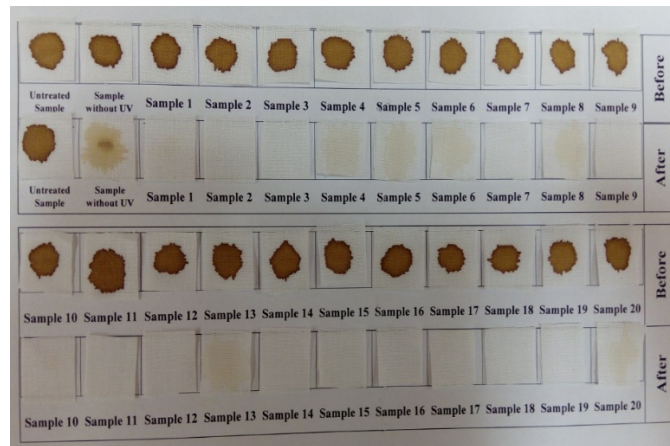


Figure 5-8 Self-cleaning efficiency after 12 h sunlight irradiations.

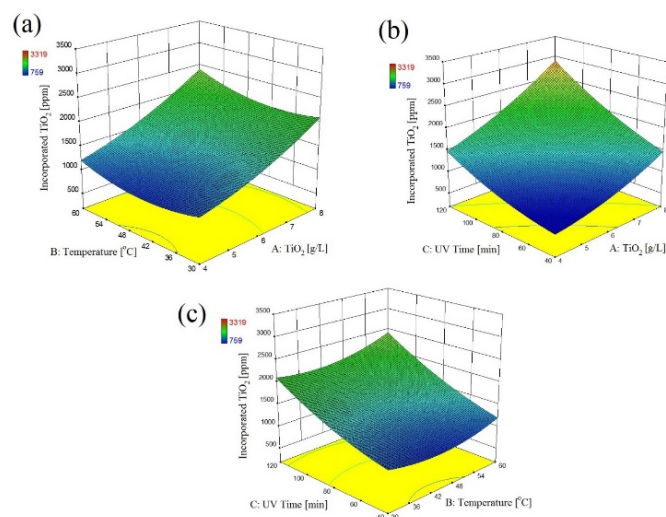


Figure 5-9 Response surfaces for incorporated amount of  $\text{TiO}_2$  NPs on cotton after UV irradiations as a function of (a)  $\text{TiO}_2$  dosage, Temperature, (b)  $\text{TiO}_2$  dosage, UV time., (c) Temperature, UV time.

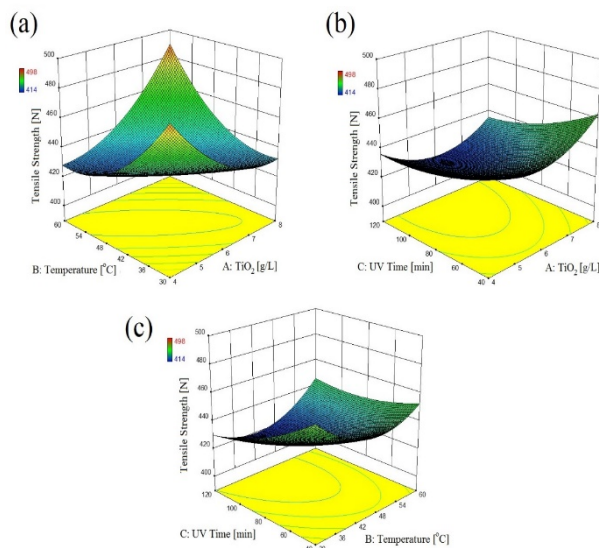


Figure 5-10 Response surfaces for tensile strength of cotton after UV irradiations as a function of (a)  $\text{TiO}_2$  dosage, Temperature, (b)  $\text{TiO}_2$  dosage, UV time., (c) Temperature, UV time.

### 5.3 Results and discussions for In-situ developed multifunctional CT nanocomposites

This section explains the results for the developed multifunctional CT nanocomposites and discusses their applications.

#### 5.3.1 SEM images and EDX spectra

The morphology of the developed CT nanocomposites was investigated by comparing SEM images of untreated cotton (blank sample), sample 9 and sample 18 as illustrated in Figure 5-11. In Figure 5-11 (a-c), SEM images are showing a smooth and clean surface of blank sample as no treatment was applied on it. Figure 5-11 (d-f) illustrates that in sample 18,  $\text{TiO}_2$  NPs were homogeneously deposited on cotton fabric by ultrasonic irradiations. Higher magnification of sample 18 was used to determine the distribution of particles on the surface of cotton as shown in Figure 5-11 (f). In Figure 5-11 (g-i), it can be seen that  $\text{TiO}_2$  NPs covered the surface of sample 9 as a condense layer and strongly aggregated.

The EDX spectrum of blank sample and sample 9 are illustrated in *Figure 5-11 (j-k)* respectively. The presence of TiO<sub>2</sub> NPs on cotton was confirmed by EDX spectrum. Moreover, the higher weight percentage of Ti element in sample 9 was indicating the higher loading of TiO<sub>2</sub> NPs. The EDX results are in good agreement with SEM results.

**Table 5-5 ANOVA results for incorporated amount of TiO<sub>2</sub> NPs on cotton after UV irradiations**

Source	Sum of Squares	df	Mean Square	F Value	p-value Prob > F	Remarks
Model	10727146	9	1191905	10592.9	< 0.0001	Significant
A-Dosage	4968441	1	4968441	44156.6	< 0.0001	Significant
B-Temperature	159844.7	1	159845	1420.6	< 0.0001	Significant
C-UV Time	4318113.3	1	4318113	38376.8	< 0.0001	Significant
AB	16020.5	1	16020.5	142.3	< 0.0001	Significant
AC	180600.5	1	180601	1605.07	< 0.0001	Significant
BC	20604.5	1	20604.5	183.1	< 0.0001	Significant
A <sup>2</sup>	399211.9	1	399212	3547.9	< 0.0001	Significant
B <sup>2</sup>	563422.6	1	563423	5007.3	< 0.0001	Significant
C <sup>2</sup>	227357.4	1	227357	2020.6	< 0.0001	Significant
Residual	1125.1	10	112.5			
Lack of Fit	902.3	5	180.4	4.05	0.075	Not significant
Pure Error	222.8	5	44.5			
Cor Total	10728271.2	19				

R-squared: 0.9999, adjusted R-squared: 0.9998, CV%: 0.62

**Table 5-6 ANOVA results for tensile strength of cotton after UV irradiations**

Source	Sum of Squares	df	Mean Square	F Value	p-value Prob > F	Remarks
Model	17334.2	9	1926.0	43.1	< 0.0001	Significant
A-Dosage	100	1	100	2.2	0.16533	Not significant
B-Temperature	1.1	1	1.1	0.02	0.87406	Not significant
C-UV Time	1678.8	1	1678.8	37.6	0.0001	Significant
AB	6272	1	6272	140.5	< 0.0001	Significant
AC	72	1	72	1.6	0.232	Not significant
BC	450	1	450	10.08	0.009	Significant
A <sup>2</sup>	6028.7	1	6028.7	135.06	< 0.0001	Significant
B <sup>2</sup>	4129.8	1	4129.8	92.5	< 0.0001	Significant
C <sup>2</sup>	472.4	1	472.4	10.5	0.008	Significant
Residual	446.3	10	44.6			
Lack of Fit	338.8	5	67.7	3.1	0.116	Not significant
Pure Error	107.5	5	21.5			
Cor Total	17780.5	19				

R-squared: 0.9749, adjusted R-squared: 0.9523, CV%: 1.47

### 5.3.2 XRD analysis

The XRD patterns for extracted solid powders are described in *Figure 5-12*. Sample C prepared by conventional stirring shows amorphous nature as no sharp peak appeared in the XRD pattern which are the characteristics of crystalline phase of developed CT nanocomposites. However, a series of crystalline peaks were obtained for all other samples developed by Ultrasonic Acoustic Method (UAM). The crystalline peaks observed at  $2\theta=25.4^\circ$ ,  $38^\circ$ ,  $48^\circ$ ,  $53.8^\circ$ ,  $55^\circ$  and  $62^\circ$  for plane reflections (101, 004, 200, 105, 211 and 204 respectively) represent the pure anatase form of TiO<sub>2</sub> NPs according to JCPDS card no 21-1272. The chief influence of ultrasonication on crystallization of TiO<sub>2</sub> NPs was experienced by comparing sample C with sample 9 (*Table 5-7*). Ultrasonic waves are the only difference between these samples as ultrasonication plays a vital role in the crystallization mechanism of the synthesis of TiO<sub>2</sub> NPs. The crystallite size of the NPs obtained from solid powder was



calculated by Scherrer's equation and reported in *Figure 5-12 (a)*. The average crystallite size of all the specimen was equal to 4 nm. The XRD analysis of sample 9 and untreated cotton (blank sample) is illustrated in *Figure 5-12 (b)*. The XRD pattern of untreated cotton (blank sample) showed only one characteristic peak at 21.3° which confirms a typical cotton fibre structure as concluded by Uddin et. al. [40].

The calculated crystallite size of the loaded TiO<sub>2</sub> NPs by *Equation 2*, was 3.982 by using FWHM at 2θ=25.4°. The XRD results confirm that the crystallite size of extracted TiO<sub>2</sub> NPs in comparison with loaded TiO<sub>2</sub> NPs on cotton fabric by Ultrasonic Acoustic Method have no significant differences.

### 5.3.3 ICP-AES elemental analysis

ICP-AES analysis of samples 1-20 developed by UAM and sample C developed by conventional stirring method confirmed the presence of TiO<sub>2</sub> NPs on treated samples. However, in blank sample, Ti element was not detected. In order to estimate the synthesized and deposited amount of TiO<sub>2</sub> NPs on cotton fabric, the characteristic peak of titanium observed in emission spectra was counted and the response was reported in *Table 5-7*. The loaded amount of TiO<sub>2</sub> NPs for sample 9 and sample C were 1587 ppm and 411 ppm respectively. More loading of TiO<sub>2</sub> NPs in sample 9 indicating the effects of ultrasonic acoustic irradiations. Moreover, a statistical study was performed to evaluate the effects of synthesis variables on deposited amount of TiO<sub>2</sub> NPs on cotton as reported in section 5.3.10.

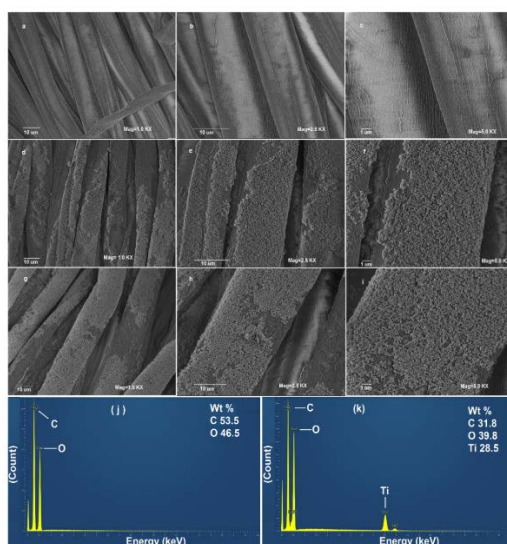
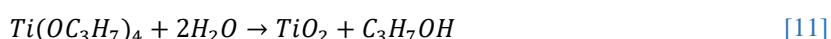
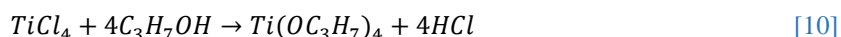


*Figure 5-11 SEM analysis of blank sample (a-c), sample 18 (d-f) and sample 9 (g-i); and EDX spectrum of blank sample (j) and sample 9 (k).*

### 5.3.4 In-situ synthesis and deposition of TiO<sub>2</sub> NPs on cotton

During In-situ process, TiO<sub>2</sub> NPs were synthesized and deposited on cotton by Ultrasonic Acoustic Method according to the following reactions as illustrated in *Equations (10-11)* [38; 43].



In ultrasonic system, an acoustic cavitation phenomenon produce a local hot spot with extreme conditions of temperature and pressure [44]. These conditions generate free H• and OH• radicals [45]. These radicals promote the reaction mechanism and generate TiO<sub>2</sub> NPs at low temperature.



### 5.3.5 UPF efficiency of CT nanocomposites

The absorption of UV radiations is a natural characteristic of TiO<sub>2</sub>. The UPF value directly evaluates the UV absorption efficiency of the synthesized samples. The high UV absorption intensity leads to higher UPF. The results of UPF efficiency are described in *Table 5-7*. The UPF values of all samples varied from 3 (blank sample) to 63 (sample 9). The results indicate that UPF values are strongly related to TiO<sub>2</sub> content deposited on textile.

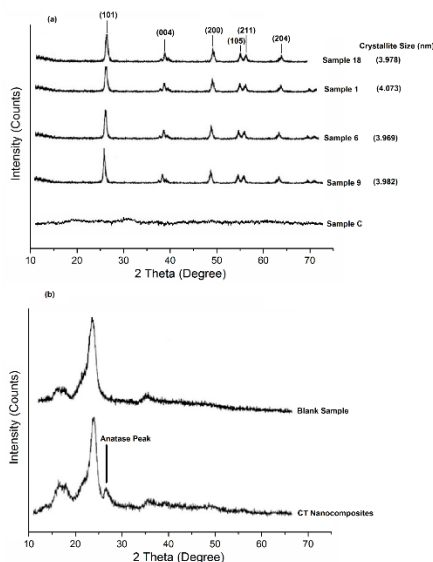


Figure 5-12 XRD pattern for (a) extracted TiO<sub>2</sub> NPs powder (b) blank sample and sample 9.

### 5.3.6 Self-cleaning efficiency of CT nanocomposites

For self-cleaning evaluation, samples were stained in 0.01 % (w/v) solution of MB and colour change was calculated for all samples after 24 h daylight irradiations and presented in *Table 5-7*. Significant change in colour was observed in case of sample 1-20 as presented in *Figure 5-13*. However, slight colour change was observed for sample C and almost no change in blank (controlled) sample. In addition, the values of  $\Delta RGB$  were higher for samples 1-20 as compared to sample C and blank sample. These results indicate the self-cleaning efficiency of CT nanocomposites synthesized by UAM was significantly higher than sample C. Higher colour difference leads to better self-cleaning efficiency that was obtained by sample 9 with optimal conditions as illustrated in *Table 5-7*.

### 5.3.7 Antimicrobial efficiency of CT nanocomposites

The antimicrobial efficiencies of the developed CT nanocomposites are presented in *Table 5-7*. Incubation of the blank sample (untreated cotton) did not show any significant effect on bacteria cells viability, even after 24 h of incubation. However, significant results were obtained for all other samples. For samples 1, 4, 8 and 18, R% against *S. aureus* and *E. coli* after 24 h contact time was more than 80 %. However, R% for sample 9 was 99 %. We observed that sample 9 exhibit excellent antimicrobial efficiency as compared to other samples including sample C. It could be possible that sample 9 possess more amount of TiO<sub>2</sub> NPs as illustrated in *Table 5-7* or the larger surface area of NPs on cotton might enhance the contact area between TiO<sub>2</sub> and bacterial cells, which may result in a higher antimicrobial efficiency. Same results were reported by Qi et al. [46]. Overall, the results showed excellent antimicrobial properties of CT nanocomposites synthesized by Ultrasonic Acoustic Method.

### 5.3.8 Washing durability of CT nanocomposites

Washing effluent analysis was used as a direct approach to evaluate washing durability. This method provides an excellent evaluation of washing durability. In a typical process, the total amount of TiO<sub>2</sub> NPs present in the effluent was considered as durability against washing. Higher concentration of TiO<sub>2</sub> NPs in effluent indicates lower durability [15]. So, the effluents were evaluated by spectrophotometer during 30 consecutive home launderings. An absorption peak at 280 nm during initial washing cycle indicating the presence of TiO<sub>2</sub> NPs as presented in *Figure 5-14* [47]. It can be possible that some of the physically attached unstable NPs were migrated into effluents during primary washing [48]. The results confirmed that no absorption peak was

observed during subsequent washing cycles showing the absence of TiO<sub>2</sub> NPs in washing effluents. Moreover, the results show that TiO<sub>2</sub> NPs are strongly attached to cotton fibres. TiO<sub>2</sub> NPs have strong affinity towards carboxyl and hydroxyl groups [49; 50].

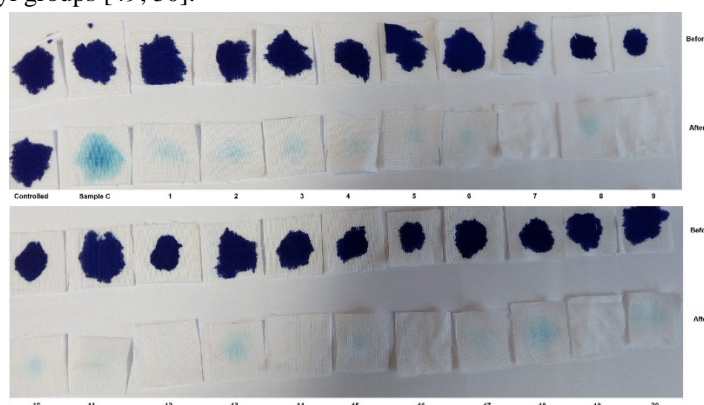


Figure 5-13 Self-cleaning efficiency of CT nanocomposites after 24 h daylight irradiations.

### 5.3.9 Tensile strength of CT nanocomposites

The results regarding breaking force for untreated cotton (blank sample) and sample 9 were 511 N and 497 N with standard deviation of 2.1 and 2.4 respectively. The results of breaking force for sample 9 were almost same with blank sample. This shows that the experimental conditions and ultrasonic irradiations did not damage the structure of cotton fibre to a significant level. The slight difference in sample 9 could be due to cleavage of cellulosic chain or by ultrasonic irradiations [34]. The results indicate that synthesis and deposition of TiO<sub>2</sub> NPs on cotton by Ultrasonic Acoustic Method have no significant damage effect to cotton fibre structure.

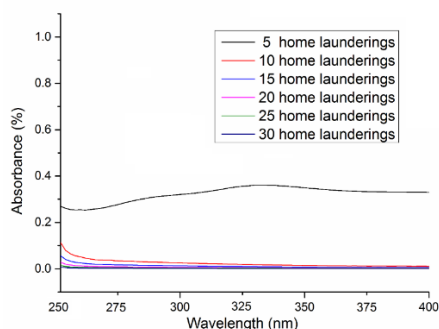


Figure 5-14 Washing effluent absorbance spectra of sample 9 after different washing cycles.

### 5.3.10 Statistical analysis of CT nanocomposites

The experimental design with different amount of TTC and ISP under varying sonication time based on the actual values of CCD for CT nanocomposites as well as sample C and blank sample (untreated cotton) is shown in **Table 5-7**. The responses of the variables including: Y<sub>3</sub>=Synthesized and deposited amount of TiO<sub>2</sub> NPs on cotton fabric; Y<sub>4</sub>=UPF of the CT nanocomposites; Y<sub>5</sub>=Self-cleaning efficiency after 24 h irradiations; Y<sub>6</sub>=Antimicrobial efficiency of the CT nanocomposites, were adjusted by **Equation 1**.

**Table 5-7** The 3-factors CCD matrix based on actual values for experimental variables and responses, Y<sub>3</sub>=Synthesized & loaded amount of TiO<sub>2</sub> NPs on cotton fabric, Y<sub>4</sub>=UPF efficiency of CT nanocomposites, Y<sub>5</sub>=Self-cleaning efficiency of CT nanocomposites, Y<sub>6</sub>=Antimicrobial efficiency of CT nanocomposites

Sample Name	TTC [mL]	ISP [mL]	Sonication time [h]	Y <sub>3</sub> =Synthesized & loaded TiO <sub>2</sub> [ppm]	Y <sub>4</sub> =UPF Efficiency [-]	Y <sub>5</sub> =Self-cleaning Efficiency [-]	Y <sub>6</sub> =Antimicrobial Efficiency [%]
Blank Sample	0	0	0	0	3	6	5
Sample C	10	6	0	411	38	61	73
1	6	4	2	830	43	83	85
2	6	4	4	839	45	85	81
3	4	2	1	749	37	70	76
4	6	4	0.25	645	44	84	85
5	6	4	2	820	43	80	80
6	6	8	2	543	40	77	79
7	8	2	3	860	47	84	83
8	8	6	1	986	50	87	87
9	10	6	2	1587	63	99	99
10	6	0.5	2	288	27	64	65
11	6	4	2	800	42	79	80
12	6	4	2	825	43	80	79
13	6	4	2	765	42	79	78
14	4	2	3	510	32	69	68
15	4	4	3	524	34	71	72
16	8	2	1	590	41	78	79
17	6	4	2	815	45	82	83
18	8	6	3	1298	58	95	94
19	4	6	1	485	37	74	73
20	2	4	2	501	25	62	65

Statistical analysis (ANOVA) was conducted to evaluate the interaction between the variables and the responses of the designed samples 1-20 and presented in *Table 5-8* to *Table 5-11*. The results indicate that the designed model for the synthesized and deposited amount of TiO<sub>2</sub> NPs on cotton is statistically significant at F-value 103.6 and p-value <0.0001 as presented in *Table 5-8*. In addition, the developed model for UPF efficiency of the developed CT nanocomposites is significant at F-value 55 and p-value <0.0001 as presented in *Table 5-9*. Moreover, the developed model for self-cleaning efficiency and antimicrobial efficiency of the developed CT nanocomposites are significant at F-value of 65.1 and 25.1 and p-value of <0.0001 and <0.0001 respectively as presented in *Table 5-10* and *Table 5-11*.

R-squared coefficient was used to evaluate the fit of the developed models. The results presented in *Table 5-8* indicate that only 1.06 % of the total variables cannot be explained through this model for synthesized and deposited amount of TiO<sub>2</sub> NPs on cotton fabric. Moreover, the results of R-squared for UPF, self-cleaning and antimicrobial efficiencies of the developed CT nanocomposites indicate that only 1.98 %, 1.68 % and 4.23 % of the total variables cannot be explained by the model respectively (*Table 5-9* to *Table 5-11*). For the evaluation of obtained results and the relationship between independent variables and response surfaces, several mathematical models (Equations 12-15) were established. In order to predict the responses for a given amount

or value of TTC and ISP and/or ultrasonic irradiation time, these models could be useful and further utilised. In [Figure 5-15](#) to [Figure 5-18](#), contour and response surface plots were drawn based on the mathematical models.

The synthesized and deposited amount of TiO<sub>2</sub> NPs on cotton according to the developed model is calculated by [Equation 12](#):

$$Y_3 = 1442.3 - 253.8(TTC) + 4.0(ISP) - 298.5(Time) + 37.7(TTC * ISP) + 59.1(TTC * Time) + 10.7(ISP * Time) + 7.2(TTC)^2 - 26.9(ISP)^2 - 14.8(Time)^2 \quad [12]$$

The UPF efficiency of the developed CT nanocomposites is calculated by [Equation 13](#):

$$Y_4 = 36.6 - 0.7(TTC) + 2.6(ISP) - 11.4(Time) + 0.6(TTC * ISP) + 1.4(TTC * Time) + 0.09(ISP * Time) - 0.07(TTC)^2 - 0.6(ISP)^2 + 0.6(Time)^2 \quad [13]$$

The self-cleaning efficiency of the developed CT nanocomposites is calculated by [Equation 14](#):

$$Y_5 = 62.1 + 1.2(TTC) + 4.7(ISP) - 10.8(Time) + 0.4(TTC * ISP) + 1.2(TTC * Time) - 0.05(ISP * Time) - 0.1(TTC)^2 - 0.7(ISP)^2 + 1.1(Time)^2 \quad [14]$$

The antimicrobial efficiency is of the developed CT nanocomposites is calculated by [Equation 15](#):

$$Y_6 = 78.0 - 0.4(TTC) + 1.9(ISP) - 12.9(Time) + 0.6(TTC * ISP) + 1.2(TTC * Time) + 0.5(ISP * Time) - 0.09(TTC)^2 - 0.6(ISP)^2 + 0.6(Time)^2 \quad [15]$$

According to the above equations and obtained results ([Table 5-7](#)), the optimal points for best possible results are 10 mL TTC, 6 mL ISP and 2 h ultrasonic irradiation time. The predicted response values for optimal conditions (Sample 9) are 1600, 63, 99 and 99 for Y<sub>3</sub>, Y<sub>4</sub>, Y<sub>5</sub> and Y<sub>6</sub> respectively.

### 5.3.11 Reusability and sequential application of CT nanocomposites

Reusability of a catalyst is a significantly important property for application point of view. The reusability of the developed CT nanocomposites was estimated by repeating their application in the photocatalytic removal of MB. The experiment was repeated for seven cycles. In each cycle, a piece of sample 9 was immersed in an aliquot of fresh MB solution. As shown in [Figure 5-19](#), after 7 reuse cycles, the removal rate of MB had lost only 7.5 % for sample 9 which was developed with optimal conditions. The results confirmed that the developed CT nanocomposites are very stable and reusable as a catalyst.

The behaviour of MB under different conditions i.e. in the presence of dark; in the presence of light only; in the presence of TiO<sub>2</sub> only; and in the presence of TiO<sub>2</sub> and light has also been evaluated and the results are presented in [Figure 5-20](#). Under dark conditions and in the absence of TiO<sub>2</sub>, the MB colour remained unchanged, while with TiO<sub>2</sub>, only 8 % change in MB colour was found. Whereas 99.6 % results were obtained with TiO<sub>2</sub> under light.

**Table 5-8 ANOVA results for synthesized and deposited amount of TiO<sub>2</sub> NPs on cotton fabric**

Source	Sum of Squares	df	Mean Square	F Value	p-value Prob > F	Remarks
Model	1613611	9	179290	103.6	< 0.0001	Significant
A-TTC	596350	1	596350	344.8	< 0.0001	Significant
B-ISP	68037.9	1	68037.9	39.3	< 0.0001	Significant
C-Sonication Time	22931.5	1	22931.5	13.2	0.004	Significant
AB	173460	1	173460	100.2	< 0.0001	Significant
AC	104852	1	104852	60.6	< 0.0001	Significant
BC	2902.06	1	2902.06	1.6	0.224	Not significant
A <sup>2</sup>	18357.3	1	18357.3	10.6	0.008	Significant
B <sup>2</sup>	233198	1	233198	134.8	< 0.0001	Significant
C <sup>2</sup>	4453.5	1	4453.5	2.5	0.139	Not significant
Residual	17294.6	10	1729.4			
Lack of Fit	14423.7	5	2884.7	5.02	0.0505	Not significant
Pure Error	2870.8	5	574.1			
Cor Total	1630906	19				

R-squared: 0.9894, adjusted R-squared: 0.9799, CV%: 5.45

**Table 5-9 ANOVA results for UPF efficiency of the developed CT nanocomposites**

Source	Sum of Squares	df	Mean Square	F Value	p-value Prob > F	Remarks
Model	1513.2	9	168.139	55	< 0.0001	Significant
A-TTC	832.1	1	832.1	272.4	< 0.0001	Significant
B-ISP	133.6	1	133.6	43.7	< 0.0001	Significant
C-Sonication Time	1.4	1	1.4	0.5	0.502	Not significant
AB	50.1	1	50.1	16.4	0.002	Significant
AC	65.8	1	65.8	21.5	0.0009	Significant
BC	0.2	1	0.2	0.07	0.796	Not significant
A <sup>2</sup>	2.07	1	2.07	0.6	0.429	Not significant
B <sup>2</sup>	130.8	1	130.8	42.8	< 0.0001	Significant
C <sup>2</sup>	7.6	1	7.6	2.5	0.144	Not significant
Residual	30.5	10	30.5			
Lack of Fit	24.5	5	4.9	4.09	0.074	Not significant
Pure Error	6	5	1.2			
Cor Total	1543.8	19				

R-squared: 0.9802, adjusted R-squared: 0.9624, CV%: 4.17

**Table 5-10 ANOVA results for self-cleaning efficiency of the developed CT nanocomposites**

Source	Sum of Squares	df	Mean Square	F Value	p-value Prob > F	Remarks
Model	1594.6	9	177.2	65.1	< 0.0001	Significant
A-TTC	884.2	1	884.2	325.2	< 0.0001	Significant
B-ISP	172.9	1	172.9	63.6	< 0.0001	Significant
C-Sonication Time	4.7	1	4.7	1.7	0.216	Not significant
AB	28.6	1	28.6	10.5	0.008	Significant
AC	43.4	1	43.4	15.9	0.002	Significant
BC	0.08	1	0.08	0.02	0.866	Not significant
A <sup>2</sup>	6.6	1	6.6	2.4	0.149	Not significant
B <sup>2</sup>	163.6	1	163.6	60.1	< 0.0001	Significant
C <sup>2</sup>	24.9	1	24.9	9.1	0.0127	Significant
Residual	27.2	10	27.2			
Lack of Fit	13.6	5	2.7	1.01	0.494	Not significant
Pure Error	13.5	5	2.7			
Cor Total	1621.8	19				

R-squared: 0.9832, adjusted R-squared: 0.9681, CV%: 2.08

**Table 5-11 ANOVA results for antimicrobial efficiency of the developed CT nanocomposites**

Source	Sum of Squares	df	Mean Square	F Value	p-value Prob > F	Remarks
Model	1341.6	9	149	25.1	< 0.0001	Significant
A-TTC	691.1	1	691.1	116.5	< 0.0001	Significant
B-ISP	139.5	1	139.5	23.5	0.0007	Significant
C-Sonication Time	3.3	1	3.3	0.5	0.4705	Not significant
AB	45.1	1	45.1	7.6	0.0201	Significant
AC	49.6	1	49.6	8.3	0.016	Significant
BC	7.2	1	7.2	1.2	0.296	Not significant
A <sup>2</sup>	2.9	1	2.9	0.4	0.498	Not significant
B <sup>2</sup>	126.6	1	126.6	21.3	0.0009	Significant
C <sup>2</sup>	8.2	1	8.2	1.3	0.265	Not significant
Residual	59.2	10	59.2			
Lack of Fit	24.4	5	4.8	0.70198	0.646	Not significant
Pure Error	34.8	5	6.9			
Cor Total	1400.9	19				

R-squared: 0.9577, adjusted R-squared: 0.9196, CV%: 3.06

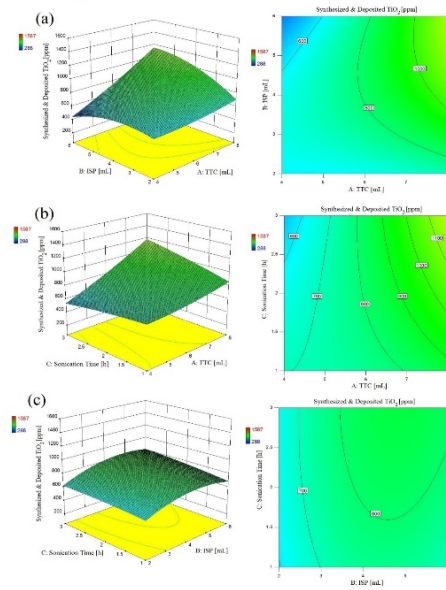


Figure 5-15 Response surfaces and contour plots for synthesized and deposited amount of  $\text{TiO}_2$  NPs on cotton as a function of (a) TTC conc., ISP conc., (b) TTC conc., Sonication time, (c) ISP conc., Sonication time.

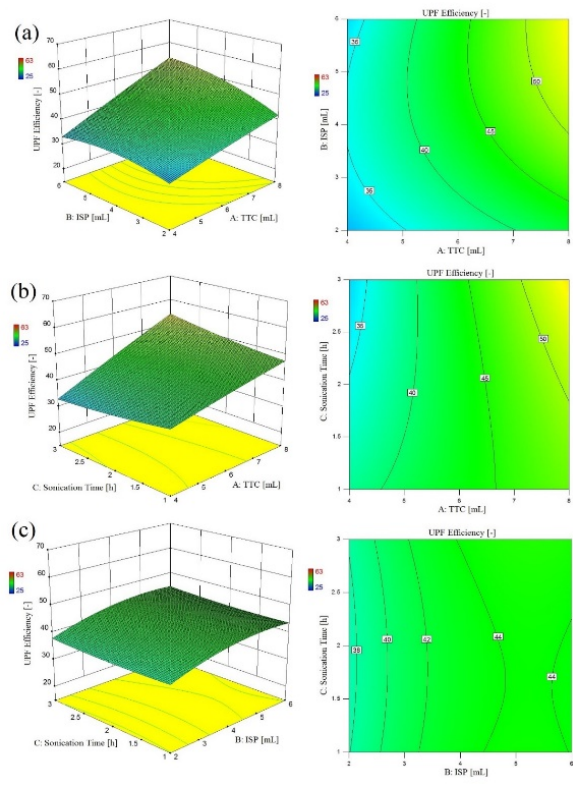


Figure 5-16 Response surfaces and contour plots for UPF efficiency of developed CT nanocomposites as a function of (a) TTC conc., ISP conc., (b) TTC conc., Sonication time, (c) ISP conc., Sonication time.



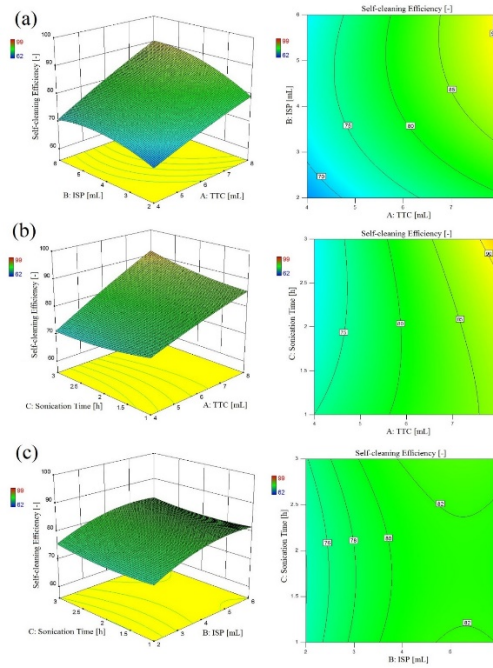


Figure 5-17 Response surfaces and contour plots for self-cleaning efficiency of developed CT nanocomposites as a function of (a) TTC conc., ISP conc., (b) TTC conc., Sonication time, (c) ISP conc., Sonication time.

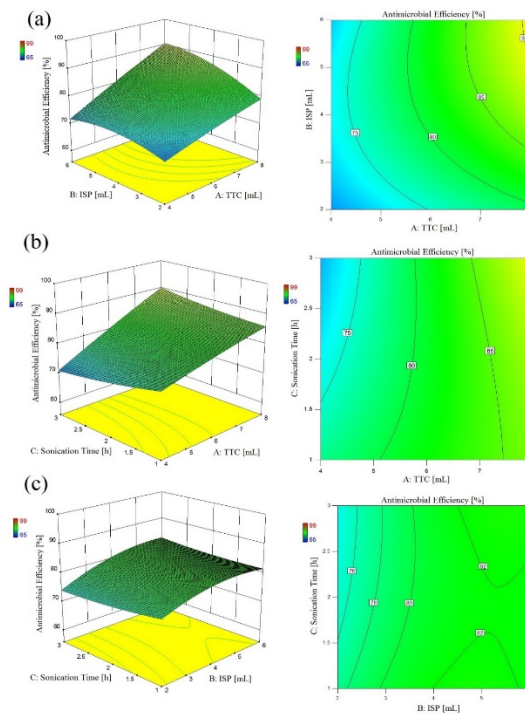


Figure 5-18 Response surfaces and contour plots for antimicrobial efficiency of developed CT nanocomposites as a function of (a) TTC conc., ISP conc., (b) TTC conc., Sonication time, (c) ISP conc., Sonication time.



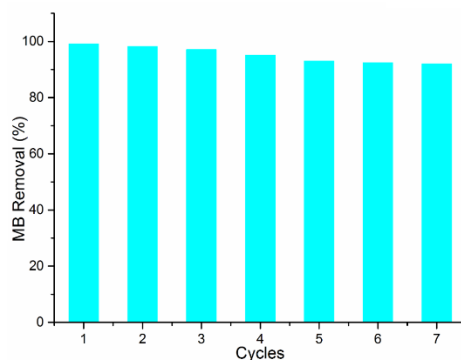


Figure 5-19 Reusability of the developed CT nanocomposites.

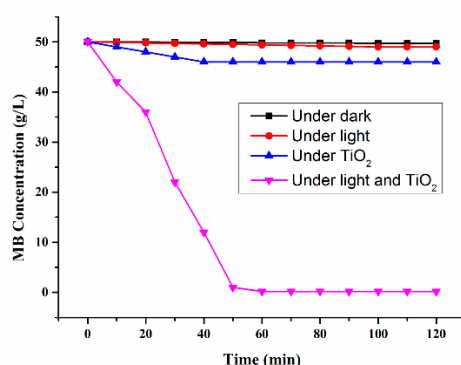


Figure 5-20 Behaviour of MB degradation under different conditions i.e. Under dark; Under light; Under TiO<sub>2</sub>; Under light and TiO<sub>2</sub>.

## 6 Evaluation of the results and new findings

The overall summary of this dissertation comprises the conclusion of the obtained results and the recommendations for future work.

### 6.1 Conclusion

After a comprehensive introduction and discussion about the related work, Chapter 4 explained the bulk of the work deriving important materials and used methods. The data was further used in Chapter 5 to perform chemical analysis and statistical calculations.

TiO<sub>2</sub> NPs (RNP) with pure anatase form were successfully synthesized by Ultrasonic Acoustic Method (UAM) using TTIP and EG as synthesis variables. The RNP were found to be more photoactive than commercially available photo catalyst P25. The average particle size for RNP was relatively small as compared to P25. The photo degradation of MB dye showed excellent dye removal ability for the RNP. The role of ultrasonic irradiations time and precursors concentration was very crucial in order to synthesize highly crystalline NPs with smaller particle and higher photocatalytic activity. The use of EG suppressed the crystal growth as well as anatase-rutile phase transformation. Self-cleaning of cotton fabrics recommends the potential use of RNP in textile industry. Reusability of the RNP confirmed their durability during photocatalytic processes. The RNP could be further utilized in many other textile applications.

In another experiment, the developed TiO<sub>2</sub> NPs were successfully embedded on cotton fabric by UV light. SEM, EDX and ICP-AES analysis confirmed the deposition of TiO<sub>2</sub> NPs on cotton. Higher incorporated amount of TiO<sub>2</sub> NPs onto cotton led to higher self-cleaning efficiency. Leaching durability of UV treated samples (samples 1 to 20) confirmed the role of UV light irradiations for the stabilization of TiO<sub>2</sub> NPs onto

cotton. Moreover, almost similar tensile strength of untreated samples and samples 1 to 20 verified the fitting of the used method. Statistical analysis confirmed that the obtained results solely rely on TiO<sub>2</sub> dosage, temperature and UV irradiations time. Optimal conditions for obtaining best possible results were attained by using 8 gL<sup>-1</sup> TiO<sub>2</sub>, 60 °C temperature and 120 min UV irradiations time.

In another study, an in-situ Ultrasonic Acoustic Method is developed to simultaneously synthesize and deposit TiO<sub>2</sub> NPs on cotton fabric in a single step. Pure anatase crystals were detected on XRD analysis indicating the crucial effects of ultrasonic irradiations at low temperature (70 °C) synthesis. In addition, more amount of TTC and prolonged sonication time led to more crystals of TiO<sub>2</sub>. SEM, EDX and ICP-AES analysis confirmed the presence of TiO<sub>2</sub> NPs on cotton. The deposited particles on cotton fabric possessed pure anatase crystals with average size 4 nm as confirmed by XRD analysis. High amount of TiO<sub>2</sub> NPs deposited on cotton led to higher functional properties such as UPF, self-cleaning and antimicrobial properties. Washing durability of the ultrasonic irradiated samples confirmed the role of acoustic cavitation and bonding between TiO<sub>2</sub> and hydroxyl groups of cotton. Moreover, ultrasonic irradiations had no negative effect on the tensile strength of the developed CT nanocomposites verifying the fitting of the used method. Statistical analysis confirmed that the obtained results solely relied on TTC concentration, ultrasonic irradiation time and ISP amount. The optimal conditions for obtaining the best results were obtained by using 10 mL TTC, 6 mL ISP and 2 h ultrasonic irradiation time.

## 6.2 Follow-up work

Working on this dissertation has uncovered many worthy avenues for future investigations. The inquisitive readers will no-doubt have ideas of their own, but there are some suggestions for research of possible interest:

- ❖ Synthesis of other metal oxides nanoparticles e.g. Fe, Zn, Cu, Ag, Au etc. through Ultrasonic Acoustic Method (UAM).
- ❖ Some other polymeric textile fibres i.e. polypropylene, polyester, polyamide can be utilized to make nanocomposites through UAM that can be more beneficial to investigate the effects of ultrasonic irradiations on different textile substrates.

## 7 References

1. DREXLER, K. E. Molecular directions in nanotechnology. *Nanotechnology*, 1991, **2** (3), 113.
2. DREXLER, K. E. Molecular tip arrays for molecular imaging and nanofabrication. *Journal of Vacuum Science & Technology B: Microelectronics and Nanometer Structures Processing, Measurement, and Phenomena*, 1991, **9** (2), 1394-1397.
3. ATEES, M. Graphene and its nanocomposites used as an active materials for supercapacitors. *Journal of Solid State Electrochemistry*, 2016, **20** (6), 1509-1526.
4. BOGART, L. K., G. POURROY, C. J. MURPHY, V. PUNTES, T. PELLEGRINO, D. ROSENBLUM, D. PEER and R. LÉVY. Nanoparticles for imaging, sensing, and therapeutic intervention. *ACS Nano*, 2014, **8** (4), 3107-3122.
5. CAI, P., W. R. LEOW, X. WANG, Y. L. WU and X. CHEN. Programmable Nano-Bio Interfaces for Functional Biointegrated Devices. *Advanced Materials*, 2017, **29** (26), 1-26.
6. NOUR, E., A. BONDAREVS, P. HUSS, M. SANDBERG, S. GONG, M. WILLANDER and O. NUR. Low-frequency self-powered footstep sensor based on ZnO nanowires on paper substrate. *Nanoscale Research Letters*, 2016, **11** (1), 1-7.
7. SAWHNEY, A., B. CONDON, K. SINGH, S. PANG, G. LI and D. HUI. Modern applications of nanotechnology in textiles. *Textile Research Journal*, 2008, **78** (8), 731-739.
8. SOLANKI, A., J. D. KIM and K.-B. LEE. Nanotechnology for regenerative medicine: nanomaterials for stem cell imaging. *Nanomedicine*, 2008, **3** (4), 567-578.
9. WANG, L., Q. XIONG, F. XIAO and H. DUAN. 2D nanomaterials based electrochemical biosensors for cancer diagnosis. *Biosensors and Bioelectronics*, 2017, **89**, 136-151.
10. YIN, J. and B. DENG. Polymer-matrix nanocomposite membranes for water treatment. *Journal of Membrane Science*, 2015, **479**, 256-275.

11. ARAIN, R. A., Z. KHATRI, M. H. MEMON and I.-S. KIM. Antibacterial property and characterization of cotton fabric treated with chitosan/AgCl–TiO<sub>2</sub> colloid. *Carbohydrate Polymers*, 2013, **96** (1), 326-331.
12. BEHZADNIA, A., M. MONTAZER, A. RASHIDI and M. MAHMOUDI RAD. Rapid Sonosynthesis of N-Doped Nano TiO<sub>2</sub> on Wool Fabric at Low Temperature: Introducing Self-cleaning, Hydrophilicity, Antibacterial/Antifungal Properties with low Alkali Solubility, Yellowness and Cytotoxicity. *Photochemistry and Photobiology*, 2014, **90** (6), 1224-1233.
13. CASCHERA, D., F. FEDERICI, T. DE CARO, B. CORTESE, P. CALANDRA, A. MEZZI, R. L. NIGRO and R. G. TORO. Fabrication of Eu-TiO<sub>2</sub> NCs functionalized cotton textile as a multifunctional photocatalyst for dye pollutants degradation. *Applied Surface Science*, 2018, **427**, 81-91.
14. DAOUD, W. A. and J. H. XIN. Nucleation and growth of anatase crystallites on cotton fabrics at low temperatures. *Journal of the American Ceramic Society*, 2004, **87** (5), 953-955.
15. DASTJERDI, R., M. MONTAZER and S. SHAHSAVAN. A novel technique for producing durable multifunctional textiles using nanocomposite coating. *Colloids and Surfaces B: Biointerfaces*, 2010, **81** (1), 32-41.
16. NOMAN, M. T., J. WIENER, J. SASKOVA, M. A. ASHRAF, M. VIKOVA, H. JAMSHAD and P. KEJZLAR. In-situ development of highly photocatalytic multifunctional nanocomposites by ultrasonic acoustic method. *Ultrasonics Sonochemistry*, 2018, **40**, 41-56.
17. PERELSHEIN, I., G. APPLEROT, N. PERKAS, G. GUIBERT, S. MIKHAILOV and A. GEDANKEN. Sonochemical coating of silver nanoparticles on textile fabrics (nylon, polyester and cotton) and their antibacterial activity. *Nanotechnology*, 2008, **19** (24), 1-6.
18. PERELSHEIN, I., G. APPLEROT, N. PERKAS, E. WEHRSCHUETZ-SIGL, A. HASMANN, G. GUEBITZ and A. GEDANKEN. CuO-cotton nanocomposite: Formation, morphology, and antibacterial activity. *Surface and Coatings Technology*, 2009, **204** (1), 54-57.
19. BAI, Y., I. MORA-SERO, F. DE ANGELIS, J. BISQUERT and P. WANG. Titanium dioxide nanomaterials for photovoltaic applications. *Chemical Reviews*, 2014, **114** (19), 10095-10130.
20. CHEN, H., C. E. NANAYAKKARA and V. H. GRASSIAN. Titanium dioxide photocatalysis in atmospheric chemistry. *Chemical Reviews*, 2012, **112** (11), 5919-5948.
21. GOKILAMANI, N., N. MUTHUKUMARASAMY, M. THAMBIDURAI, A. RANJITHA and D. VELAUTHAPILLAI. Basella alba rubra spinach pigment-sensitized TiO<sub>2</sub> thin film-based solar cells. *Applied Nanoscience*, 2014, **5** (3), 297.
22. XU, M., Y. WANG, J. GENG and D. JING. Photodecomposition of NO<sub>x</sub> on Ag/TiO<sub>2</sub> composite catalysts in a gas phase reactor. *Chemical Engineering Journal*, 2017, **307**, 181-188.
23. MESKIN, P. E., V. K. IVANOV, A. E. BARANTCHIKOV, B. R. CHURAGULOV and Y. D. TRETAYAKOV. Ultrasonically assisted hydrothermal synthesis of nanocrystalline ZrO<sub>2</sub>, TiO<sub>2</sub>, NiFe<sub>2</sub>O<sub>4</sub> and Ni<sub>0.5</sub> Zn<sub>0.5</sub> Fe<sub>2</sub>O<sub>4</sub> powders. *Ultrasonics Sonochemistry*, 2006, **13** (1), 47-53.
24. SADR, F. A. and M. MONTAZER. In-situ sonosynthesis of nano TiO<sub>2</sub> on cotton fabric. *Ultrasonics Sonochemistry*, 2014, **21** (2), 681-691.
25. CHENG, Q., C. LI, V. PAVLINEK, P. SAHA and H. WANG. Surface-modified antibacterial TiO<sub>2</sub>/Ag<sup>+</sup> nanoparticles: preparation and properties. *Applied Surface Science*, 2006, **252** (12), 4154-4160.
26. HEBEISH, A., M. ABDELHADY and A. YOUSSEF. TiO<sub>2</sub> nanowire and TiO<sub>2</sub> nanowire doped Ag-PVP nanocomposite for antimicrobial and self-cleaning cotton textile. *Carbohydrate Polymers*, 2013, **91** (2), 549-559.
27. KARIMI, L., M. E. YAZDANSHENAS, R. KHAJAVI, A. RASHIDI and M. MIRJALILI. Optimizing the photocatalytic properties and the synergistic effects of graphene and nano titanium dioxide immobilized on cotton fabric. *Applied Surface Science*, 2015, **332**, 665-673.
28. LONG, M., L. ZHENG, B. TAN and H. SHU. Photocatalytic self-cleaning cotton fabrics with platinum (IV) chloride modified TiO<sub>2</sub> and N-TiO<sub>2</sub> coatings. *Applied Surface Science*, 2016, **386**, 434-441.
29. SUN, Y. and Y. XIA. Shape-controlled synthesis of gold and silver nanoparticles. *Science*, 2002, **298** (5601), 2176-2179.

30. SUN, Y., Y. YIN, B. T. MAYERS, T. HERRICKS and Y. XIA. Uniform silver nanowires synthesis by reducing AgNO<sub>3</sub> with ethylene glycol in the presence of seeds and poly (vinyl pyrrolidone). *Chemistry of Materials*, 2002, **14** (11), 4736-4745.
31. KHUSHALANI, D., G. A. OZIN and A. KUPERMAN. Glycometallate surfactants. Part 1: non-aqueous synthesis of mesoporous silica. *Journal of Materials Chemistry*, 1999, **9** (7), 1483-1489.
32. SCOTT, R. W., N. COOMBS and G. A. OZIN. Non-aqueous synthesis of mesostructured tin dioxide. *Journal of Materials Chemistry*, 2003, **13** (4), 969-974.
33. ABIDI, N., E. HEQUET, S. TARIMALA and L. L. DAI. Cotton fabric surface modification for improved UV radiation protection using sol-gel process. *Journal of Applied Polymer Science*, 2007, **104** (1), 111-117.
34. PERELSHTEIN, I., G. APPLEROT, N. PERKAS, J. GRINBLAT and A. GEDANKEN. A One-Step Process for the Antimicrobial Finishing of Textiles with Crystalline TiO<sub>2</sub> Nanoparticles. *Chemistry-A European Journal*, 2012, **18** (15), 4575-4582.
35. GASHTI, M. P. and A. ALMASIAN. UV radiation induced flame retardant cellulose fiber by using polyvinylphosphonic acid/carbon nanotube composite coating. *Composites Part B: Engineering*, 2013, **45** (1), 282-289.
36. GASHTI, M. P., A. ELAHI and M. P. GASHTI. UV radiation inducing succinic acid/silica-kaolinite network on cellulose fiber to improve the functionality. *Composites Part B: Engineering*, 2013, **48**, 158-166.
37. HUANG, W., X. TANG, Y. WANG, Y. KOLTYPIN and A. GEDANKEN. Selective synthesis of anatase and rutile via ultrasound irradiation. *Chemical Communications*, 2000, (15), 1415-1416.
38. GUO, W., Z. LIN, X. WANG and G. SONG. Sonochemical synthesis of nanocrystalline TiO<sub>2</sub> by hydrolysis of titanium alkoxides. *Microelectronic Engineering*, 2003, **66** (1), 95-101.
39. GHOWS, N. and M. H. ENTEZARI. Ultrasound with low intensity assisted the synthesis of nanocrystalline TiO<sub>2</sub> without calcination. *Ultrasonics Sonochemistry*, 2010, **17** (5), 878-883.
40. UDDIN, M., F. CESANO, F. BONINO, S. BORDIGA, G. SPOTO, D. SCARANO and A. ZECCHINA. Photoactive TiO<sub>2</sub> films on cellulose fibres: synthesis and characterization. *Journal of Photochemistry and Photobiology A: Chemistry*, 2007, **189** (2), 286-294.
41. LESSAN, F., M. MONTAZER and M. MOGHADAM. A novel durable flame-retardant cotton fabric using sodium hypophosphite, nano TiO<sub>2</sub> and maleic acid. *Thermochimica Acta*, 2011, **520** (1), 48-54.
42. NOMAN, M. T., J. MILITKY, J. WIENER, J. SASKOVA, M. A. ASHRAF, H. JAMSHAI and M. AZEEM. Sonochemical Synthesis of Highly Crystalline Photocatalyst For Industrial Applications. *Ultrasonics*, 2018, **83**, 203-213.
43. PRASAD, K., D. PINJARI, A. PANDIT and S. MHASKE. Phase transformation of nanostructured titanium dioxide from anatase-to-rutile via combined ultrasound assisted sol-gel technique. *Ultrasonics Sonochemistry*, 2010, **17** (2), 409-415.
44. PATIL, M. N. and A. B. PANDIT. Cavitation-a novel technique for making stable nano-suspensions. *Ultrasonics Sonochemistry*, 2007, **14** (5), 519-530.
45. BANG, J. H. and K. S. SUSLICK. Applications of ultrasound to the synthesis of nanostructured materials. *Advanced Materials*, 2010, **22** (10), 1039-1059.
46. QI, K., W. A. DAOUD, J. H. XIN, C. MAK, W. TANG and W. CHEUNG. Self-cleaning cotton. *Journal of Materials Chemistry*, 2006, **16** (47), 4567-4574.
47. REDDY, K. M., C. G. REDDY and S. MANORAMA. Preparation, characterization, and spectral studies on nanocrystalline anatase TiO<sub>2</sub>. *Journal of Solid State Chemistry*, 2001, **158** (2), 180-186.
48. MONTAZER, M., F. ALIMOHAMMADI, A. SHAMEI and M. K. RAHIMI. Durable antibacterial and cross-linking cotton with colloidal silver nanoparticles and butane tetracarboxylic acid without yellowing. *Colloids and Surfaces B: Biointerfaces*, 2012, **89**, 196-202.
49. DAOUD, W. A., S. LEUNG, W. TUNG, J. XIN, K. CHEUK and K. QI. Self-cleaning keratins. *Chemistry of Materials*, 2008, **20** (4), 1242-1244.
50. PAKDEL, E. and W. A. DAOUD. Self-cleaning cotton functionalized with TiO<sub>2</sub>/SiO<sub>2</sub>: focus on the role of silica. *Journal of Colloid and Interface Science*, 2013, **401**, 1-7.

## 8 List of papers published by the author

### 8.1 Publications in impact factor journals

1. M.T. Noman, J. Wiener, J. Saskova, M.A. Ashraf, M. Vikova, H. Jamshaid, P. Kejzlar, "In-situ development of highly photocatalytic multifunctional nanocomposites by ultrasonic acoustic method". *Ultrasonics Sonochemistry*, 40 (2018), 41-56. **Impact factor: 6.012.**
2. M.T. Noman, J. Militky, J. Wiener, J. Saskova, M.A. Ashraf, H. Jamshaid, M. Azeem, "Sonochemical synthesis of highly crystalline photocatalyst for industrial applications". *Ultrasonics*, 83 (2018), 203-213. **Impact factor: 2.377.**
3. M.T. Noman, M.A. Ashraf, H. Jamshaid, A. Ali, A novel green stabilization of TiO<sub>2</sub> nanoparticles onto cotton, *Fibers and Polymers*, (Accepted). **Impact factor: 1.353.**
4. H. Jamshaid, R. Mishra, J. Militky, M. Pechociakova, M.T. Noman, "Mechanical, thermal and interfacial properties of green composites from basalt and hybrid woven fabrics". *Fibers and Polymers*, 17 (2016), 1675-1686. **Impact factor: 1.353.**
5. H. Jamshaid, R. Mishra, J. Militky, M.T. Noman, "Interfacial Performance and Durability of Textile Reinforced Concrete". *The Journal of the Textile Institute*, 109 (2017), 879-890. **Impact factor: 1.174.**
6. A. Ali, N.H.A. Nguyen, V. Baheti, M. Ashraf, J. Militky, T. Mansoor, M.T. Noman, S. Ahmad, "Electrical conductivity and physiological comfort of silver coated cotton fabrics". *The Journal of the Textile Institute*, 109 (2017), 620-628. **Impact factor: 1.174.**
7. M.A. Ashraf, J. Wiener, A. Farooq, J. Saskova, M.T. Noman, "Development of Maghemite Glass Fibre Nanocomposite for Adsorptive Removal of Methylene Blue". *Fibers and Polymers*, 19 (2018), 1735-1746. **Impact factor: 1.353.**
8. M.T. Noman, M.A. Ashraf, H. Jamshaid, A. Ali, Synthesis and Applications of Nano TiO<sub>2</sub>: A Review, *Environmental Science and Pollution Research*, (Under Review). **Impact factor: 2.80.**
9. M.A. Ashraf, J. Wiener, A. Farooq, M.T. Noman, J. Saskova, S. Naeem, "Selective synthesis of iron oxide nanoparticles for efficient adsorption of methylene blue". *Desalination and Water Treatment*, (Under Review). **Impact factor: 2.327.**

### 8.2 Contributions in international conferences

1. M.T. Noman, J. Wiener, J. Saskova, M.A. Ashraf, H. Jamshaid., "Synthesis and characterization of highly crystalline anatase form titania by ultrasonic cavitation method". 8th International Textile, Clothing & Design Conference, October 02<sup>nd</sup> to 05<sup>th</sup> 2016, Dubrovnik, Croatia.
2. M.A. Ashraf, J. Wiener, M.S. Naeem, M.T. Noman., "Synthesis and application of iron oxide nanoparticles for efficient adsorption of acid red dye from water". 8th International Conference on Nanomaterials - Research and Application, NANOCON 2016; Hotel Voronez IBrno; Czech Republic; 19 October 2016 through 21 October 2016; Code 126915.
3. H. Jamshaid, R. Mishra, M.T. Noman., "Effect of basalt nanoparticles on mechanical and thermal characterization". 8th International Conference on Nanomaterials - Research and Application, NANOCON 2016; Hotel Voronez IBrno; Czech Republic; 19 October 2016 through 21 October 2016; Code 126915.
4. N.A. Jamil, B. Shahbaz, M.T. Noman., "Performance Evaluation of Ultrasonic Assisted Reactive Dyeing of Cotton Under Multiple Variables". The Fiber Society Spring 2010, International Conference, May 12-14, 2010. Merinos Congress Center, Bursa, Turkey.

### 8.3 Book chapters

1. "Synthesis and Characterization of Anatase Phase Nanoparticles". **Advances in Fibrous Material Science.**
2. "New generation of flame-resistant woven fabrics from green material". **Advances in Fibrous Material Science.**

## 8.4 Citations

**Article:** M.T. Noman, J. Wiener, J. Saskova, M.A. Ashraf, M. Vikova, H. Jamshaid, P. Kejzlar, “In-situ development of highly photocatalytic multifunctional nanocomposites by ultrasonic acoustic method”. *Ultrasonics Sonochemistry*, 40 (2018), 41-56.

(Cited in)

1. Cheng, L. et al., “Ultrasonic-assisted in-situ fabrication of BiOBr modified Bi<sub>2</sub>O<sub>2</sub>CO<sub>3</sub> microstructure with enhanced photocatalytic performance”. *Ultrasonics Sonochemistry*, 44 (2018), 137-145.
2. Guimarães, A.R. et al., “Use of ultrasound to modify the pyrolyzed biomass of Pinus spp. and the implications for biological models”. *Information Processing in Agriculture*, 5 (2018), 199-204.
3. Guan, W. et al., “Ti<sub>4</sub>O<sub>7</sub>/g-C<sub>3</sub>N<sub>4</sub> visible light photocatalytic performance on hypophosphite oxidation: Effect of annealing temperature”. *Frontiers in Chemistry*, 6 (2018), 1-11.

## Resume



**MUHAMMAD TAYYAB NOMAN M.Sc**  
**15<sup>th</sup> Feb 1986, Pakistan**

### Vision & Skills

- An enthusiastic, adaptive and fast-learning individual with a broad and acute interest in textiles, nanocomposites, ultrasonics and discovery of new innovations
- I particularly enjoy collaborating with scientists from different disciplines to develop new skills and solve new challenges

### Education

**PhD** (Textile Engineering) **Continue**  
Technical University of Liberec, **Czech Republic**

**MSc** (Fibre Technology) **2009**  
University of Agriculture, Faisalabad, **Pakistan**

### Languages

**English:** Professional proficiency  
**Urdu:** Native proficiency  
**Punjabi:** Native proficiency

### Personal Info

**Email:** tayyab\_noman411@yahoo.com  
**Mobile:** 00420-776396302  
**Country of stay:** Czech Republic  
**Nationality:** Pakistani

### Publications

M.T. Noman, J. Wiener, J. Saskova, M.A. Ashraf, M. Vikova, H. Jamshaid, P. Kajzlar., “In-situ development of highly photocatalytic multifunctional nanocomposites by ultrasonic acoustic method”, *Ultrasonics Sonochemistry*, 40 (2018), 41-56. **Impact factor: 6.012**

M.T. Noman, J. Militky, J. Wiener, J. Saskova, M.A. Ashraf, H. Jamshaid, M. Azeem., “Sonochemical synthesis of highly crystalline photocatalyst for industrial applications”, *Ultrasonics* 83 (2018), 203-213. **Impact factor: 2.377**

### Conference Papers

Muhammad Tayyab Noman, Jakub Wiener, Jana Saskova, Muhammad Azeem Ashraf, Hafsa Jamshaid., “Synthesis and characterization of highly crystalline anatase form titania by ultrasonic cavitation method”. 8th International Textile, Clothing & Design Conference, October 02<sup>nd</sup> to 05<sup>th</sup> 2016, Dubrovnik, Croatia.

Muhammad Azeem Ashraf, Jakub Wiener, Muhammad Salman Naeem, Muhammad Tayyab Noman., “Synthesis and application of iron oxide nanoparticles for efficient adsorption of acid red dye from water”. 8th International Conference on Nanomaterials - Research and Application, NANOCON 2016; Hotel Voronez IBrno; Czech Republic; 19 October 2016 through 21 October 2016; Code 126915.

## Record of the state doctoral exam



### ZÁPIS O VYKONÁNÍ STÁTNÍ DOKTORSKÉ ZKOUŠKY (SDZ)

*Jméno a příjmení doktoranda:* **Muhammad Tayyab Noman, M.Sc.**  
*Datum narození:* **15. 2. 1986**  
*Doktorský studijní program:* **Textilní inženýrství**  
*Studijní obor:* **Textile Technics and Materials Engineering**  
*Forma:* **prezenční**  
*Termín konání SDZ:* **25. 6. 2018**

**prospěl**

~~**neprospěl**~~

*Komise pro SDZ:*

*Podpis*

Předseda:	prof. RNDr. David Lukáš, CSc.
Místopředseda:	doc. Ing. Maroš Tunák, Ph.D.
Členové:	prof. Dr. Ing. Miroslav Černík, CSc.
	prof. Dr. Ing. Pavel Němeček
	doc. Ing. Petr Exnar, CSc.
	doc. Ing. Antonín Kuta, CSc.
	doc. Ing. Michal Vik, Ph.D.

V Liberci dne 25. 6. 2018

*O průběhu SDZ je veden protokol.*





## Recommendation of the supervisor



### Supervisor's thesis's evaluation for the PhD Thesis of Mr. Muhammad Tayyab Noman, M.Sc.

Title of Thesis:

#### **Stabilization of sono synthesized photocatalyst on textiles and development of multifunctional nanocomposites**

Presented dissertation thesis is about synthesis and stabilization of a novel photocatalyst to enhance the functional properties of textile. The novel cotton – TiO<sub>2</sub> multifunctional nanocomposites prepared in situ by Ultrasonic Acoustic Method was introduced. Highly photoactive anatase form of TiO<sub>2</sub> nanoparticles have been synthesized and incorporated on cotton simultaneously by this method. Functional properties of composites prepared by Ultrasonic Acoustic Method are durable against to repetitive washing, which can be supported by acoustic cavitation.

The candidate has done all work systematically on required scientific level with specific objectives. Discussion of the results is comprehensive and logical. The quality of tables and figures is good and untestable. The conclusions of the thesis are interesting and novel.

Publication activities are in very good level. During his research work on PhD theme he has published 9 papers in impact factor journals, 2 book chapter and 4 publications at international conferences.

**I recommend the thesis for final defense.**

Liberec 10/09/2018

Ing. Jana Šašková, Ph.D.  
(Supervisor)



## Opponent's reviews

Referee's report on PhD. thesis of

**Muhammad Tayyab Noman, M.Sc.**

### **„Stabilization of sono synthesized photocatalyst on textiles and development of multifunctional nanocomposites “**

*Professor Miroslav Černík*

---

The presented thesis consists of 118 pages divided into 5 major chapters all including References and List of Publications. The thesis deals with preparation of TiO<sub>2</sub> nanoparticles, their stabilization on cotton and their characterization. Chapter 1 is an introduction to the problem, chapter 2 summarizes state of the art, chapter 3 is about used materials and methods and chapter 4 discussed results, which are afterwards summarizes in the chapter 5.

#### ***List of Abbreviation***

List of abbreviation at the beginning of the thesis shows imperfections which later appears in the whole Ph.D. thesis. The list is not alphabetically arranged, trivial units (members of SI units) are evident and should not be included, “j” for joule instead of “J” is used....

#### ***Introduction***

This part starts is overall description of the problem – synthesis of TiO<sub>2</sub> nanoparticles and their fabrication in textile. The chapter also specifies research objectives and outlines. My recommendation is, if you define the abbreviation, use it! Do not define it repeatedly.

#### ***Chapter 2***

deals with overview of the current state of problem. This part is not problematic. There is enough of literature sources and up-to-date literature is used.

#### ***Chapter 3***

deals with materials and methods. Here problematic parts start. Why do you repeat table like 3-2 (3-4, 3-6) if the table content is the same? What is the  $\alpha$  value, which is not defined? Is it the standard deviation? Why do you use brackets in formulas (3, 7), where they are not needed.

Whats is source of Figure 3-5? Do photons turning?

#### ***Chapter 4***

deals with results and discussions. As I understand, 3-factors CCD matrix defines experimental variables for TTIP, EG, Time (Table 3-1). TTIP has values of 4, 6 and 8, but in Fig. 4-1 and later the optimal TTIP value is 10 mL. How is it possible?

In chapter 4.1.3. the resulting NP (RNP) are formed, but why the CCD matrix table (4-2) is different form table 3-2, which defined parameters for NP formation?

**Eq.8 (page 42) is statistically correct, but it has no physical meaning. It is just game with the numbers (fitting exercise) and I think Ph.D. student should be able to understand the nature of the processes and try to interpret the results based on physical phenomena.**

I think, graphical interpretation of the results in Figure 4-8 is wrong. Firstly, according to above mentioned statement, the optimal value of TTIP is 10, but this value is not used here. Why? Please, tell me a value for left-bottom corner of Fig 4-8c from the measurement and compare it with value in the graph. Similarly for both right corners of Fig 4-8b. I think the differences between plotted values and real results are bigger than 10%. It is in contrast with value in the table and plotted in Fig 4-9.

Also, pls, could you calculate the Predicted value in Table 4-2 for the line 7 (8, 3, 3). Is it really 91%?

What is the unit in Table 4-4?

Washing durability chapter speaks about absorption peak at 289 nm. Figure 4-15 shows major peak at about 320 nm. Why?

Pls, could you calculate  $Y_1$ =Incorporated TiO<sub>2</sub> on cotton for sample No.1 and 3 (according to eq.9) and compare it with measured values in Table 4-5? Why there are such big differences? Why there are no differences in Table 4-19 for these values?

Degradation studies. Is it based on single values only? Did you study repeated experiments to estimate experimental error?

### **Chapter 5**

Conclusion summarizes all results of Ph.D. work. In the part, where results of NPs stabilized on cotton are recapitulated, covalent bonding of NPs on cotton is mentioned. Have you any evidence of covalent binding?

### **Referee remarks, question and conclusions**

#### **QUESTIONS (repetition of above mentioned questions):**

1. What is the  $\alpha$  value in tables 3-2, 3-4, 3-6? Is it standard deviation?
2. The optimal TTIP value is 10 mL. Is it inside of CCD matrix defines experimental variables for TTIP, EG, Time (Table 3-1)?
3. Have you physical interpretation of the results, not only fitting exercise?
4. Calculate the value for left-bottom corner of Fig 4-8c and compare it with value in the graph. Similarly for both right corners of Fig 4-8b.
5. Recalculate the Predicted value in Table 4-2 for line 7 (8, 3, 3). Is it 91%?
6. What are the units in Table 4-4?
7. Washing durability chapter speaks about absorption peak at 289 nm. Figure 4-15 shows major peak at about 320 nm. Why?
8. Calculate  $Y_1$ =Incorporated TiO<sub>2</sub> on cotton for sample No.1 and 3 (according to eq.9) and compare it with measured values in Table 4-5?

#### **Referee's conclusion**

The presented thesis of Muhammad T. Noman has all necessary parts required for appropriate dissertation thesis. But, the thesis shows just fitting exercise of the results without effort to

physically understand the problem, influence of variables and interpret the results in bigger context. According to my opinion, there are also mistakes and errors. So, I think the quality of thesis is very disputable and the candidate should answer all question and try to convince the board about quality of his work.

**So, I recommend the thesis for a defence with significant doubts.**

In Liberec (Czech R.) on April 13, 2019

**Professor Miroslav Černík**

## Oponentský posudek disertační práce.

Autor práce: *Muhammad Tayyab Noman, M.Sc.*

Název práce: *Stabilization of Sono Synthesized Photocatalyst on Textiles and Development of Multifunctional Nanocomposites.*

Předložená disertační práce se zabývá stále aktuálním fenoménem, jakým je fotokatalytický efekt nanočástic některých oxidů kovů – tomto případě oxidu titaničitého.

V rozsáhlé rešeršní části shrnul doktorand dosavadní základní poznatky o studovaném jevu. Ze 135 citovaných prací byla, až na nepatrné výjimky, podstatná většina publikována po roce 2000, což svědčí o stálé aktuálnosti řešené problematiky.

V rámci experimentálních prací byla především provedena syntéza nanočástic oxidu titaničitého za vhodných podmínek. Byly získány nanočástice oxidu titaničitého v krystalové modifikaci čistého anatasu. Velikost těchto nanočástic byla cca 4 nm, pro srovnání s komerčním produktem Degussa P25, který má velikost cca 20 nm. Menší velikost syntetizovaných částic se příznivě projevila i při hodnocení jejich fotokatalytického účinku.

Bavlněná tkanina byla upravena syntetizovanými nanočásticemi dvojím způsobem. V prvním případě byla suspenze nanočástic nanosená na bavlněnou tkaninu klocovacím postupem a následně byly částice  $\text{TiO}_2$  na tkanině fixovány působením UV záření. Ve druhém případě byla syntéza nanočástic  $\text{TiO}_2$  provedena bezprostředně na bavlněné tkanině - nanokompozit.

Jak samotné částice, tak připravené „nanokompozity“ byly studovány řadou fyzikálních i fyzikálně-chemických metod, které potvrzují především velikost připravených nanočástic i jejich krystalovou modifikaci. Velmi zajímavá je vysoká stálost v praní s ohledem na množství nanočástic  $\text{TiO}_2$  na vzorku připraveném dodatečným nánosem nanočástic a jejich fixací UV zářením. Zde mohly být alespoň naznačeny zmíněné možné interakce nanočástic  $\text{TiO}_2$  s hydroxylovými skupinami celulózy.

Fotokatalytická – samočisticí - účinnost nanočástic  $\text{TiO}_2$  byla hodnocena na roztoku methylenové modře v porovnání s komerčním produktem P25 – příznivý vliv zmenšujících se nanočástic je zjevný.

Obdobnému analytickému hodnocení i „samočisticím“ schopnostem byly podrobeny vzorky bavlny dodatečně upravení nanočásticemi  $\text{TiO}_2$ . I v tomto případě komerční vzorek P25 vykazoval nižší účinnost.

Srovnatelných výsledků s předchozí variantou bylo dosaženo i při hodnocení „nanokompozitu“ kde byl také ověřován jeho antimikrobiální efekt vůči dvěma druhům mikroorganismů: *Staphylococcus aureus* a *Escherichia coli*. U obou mikroorganismů byla prokázána jejich snížená viabilita na povrchu upraveném nanočásticemi  $\text{TiO}_2$ .

Antimikrobiální účinnost by bylo možno studovat i klasickými metodami používanými v mikrobiologii. Tyto způsoby hodnocení však zcela neodpovídá předpokládanému způsobu použití textilií upravených nanočásticemi.

K práci mám některé dotazy a připomínky, které mohou být diskutovány v průběhu obhajoby.

1. Bylo by možné metodu pro přípravu nanočástic  $\text{TiO}_2$  použitou v dizertační práci po určité modifikaci použít i pro průmyslovou výrobu tohoto produktu?
2. Je reálná průmyslová výroba bavlněných tkanin (nebo tkanin z jiných materiálů, nebo netkaných textilií) dodatečně upravených nanášením nanočástic  $\text{TiO}_2$  ?
3. Jaká je možnost degradace nosných tkanin fotokatalytickým účinkem nanesených nanočástic při dlouhodobém osvětlení při aplikaci?
4. V reálných podmínkách je znečištění povrchů mnohem komplikovanější, vedle organických sloučenin (tuk, barviva) přibývají také anorganické pigmenty (saze, silikáty, uhličitany apod.).
5. Jaký je předpokládaný účinek studovaných nanočástic na lidský organismus?

Celkově je dizertační práce zpracována na velmi dobré odborné i formální úrovni. Za významné pokládám tu skutečnost, že byly vyvinuty dva matematické modely pro aplikaci  $\text{TiO}_2$  na bavlnu a pevnost v tahu bavlny po UV ozáření. Modely byly dále použity k potvrzení získaných výsledků.

Dizertační práce představuje velký objem dobře provedené a vyhodnocené experimentální práce. Zajímavá je i myšlenka v započaté práci pokračovat – především ve studiu nanočástic oxidů jiných kovů a jejich nanášení a fixaci na jiné typy tkanin.

Doktorand prokázal schopnost samostatné a systematické vědecké práce, výsledky zpracovat a předložit odborné veřejnosti formou publikací i přednášek na konferencích. Základní poznatky byly publikovány v prestižních odborných časopisech s vysokým impakt faktorem (viz. Seznam publikací).

Práce splňuje všechny nároky na ni kladené, doporučuji ji k obhajobě.

doc. Ing. Ladislav Burgert, CSc.

Ústav chemie a technologie makromolekulárních látek.

Fakulta chemicko-technologická.

Univerzita Pardubice.

Pardubice, 6. února 2019.